CHAPTER

13

Volcano Seismology

Joachim Wassermann

13.1 Introduction

Volcanic eruptions and their impact on human society, following earthquakes and meteorological disasters, are the most severe natural hazards. Since the pioneering works of Omori (1911), Sassa (1936) and Imbo (1954), much attention was focused on the seismic signals preceding or accompanying a volcanic eruption. Soon after the start of more extensive seismic monitoring it became clear that volcanoes show a variety of different seismic signals which often differ from those produced by common tectonic earthquake sources, i.e., double-couple type sources.

Starting with the availability of small portable seismographs in the late 1960s to early 1970s, a tremendous number of observations were made at different volcanoes and during different stages of activity. At the same time, first attempts were made to explain some of the seismic signals recorded and to classify the different signals by their proposed (but still mostly unknown) source mechanisms. Following this very enthusiastic period, the progress in the study of accelerated magma transport to the surface stagnated. Too many open questions remained unsolved, such as the mostly unknown source mechanisms of volcanic signals, the influence of the topography of volcanoes, the problem of proper hypocenter determination, the relationship between the occurrence of seismic signals of different type, and the associated surface activity of a volcano. Since the late 1980s to early 1990s the use of portable and robust broadband seismometers and newly developed low power consuming 24bit A/D converters, as well as the extensive use of seismic array techniques, opened new horizons and different views on the source mechanisms and the importance of volcano-seismic signals in the framework of early warning.

This Chapter should be seen as a guideline for establishing a seismic monitoring network or at least a temporary experiment at an active volcano. Because of the large number of different volcanoes and many different kinds of source mechanisms which may produce seismic signals, a description of all aspects is not possible. Also, a comprehensive review of case studies, including the variety of volcanic earthquake sequences, is beyond the scope of this paper. Relevant references include the excellent text books *Encyclopedia of Volcanoes* (Sigurdsson, 2000) and *Monitoring and Mitigation of Volcano Hazards* (Scarpa and Tilling, 1996). Most of the relevant topics dealt with in these text books are summarized below.

13.1.1 Why a different Chapter?

Volcano seismology uses many terms and methods known in earthquake seismology. This is no surprise as the same instruments and the same mechanism of elastic wave propagation through the Earth are used to investigate the subsurface structure and the activity state of a volcano. However, there are some deviations from conventional earthquake seismology, both in the physics of the signals and the methods of analyzing them. As outlined below, the signals vary from "earthquake-like" transients to long-lasting and continuous "tremor" signals. The most striking differences between earthquake and volcano seismology are the proposed source mechanisms and the related analysis techniques. In 13.2 and 13.4 we will discuss some of these aspects.

When setting up an earthquake monitoring network an optimal station coverage is needed in order to locate the events precisely. Depending on the tasks of the network, at least some stations should be located as close as possible to the active volcanic area in order to model the related seismic source with sufficient accuracy and determine the source depth. Hence, we are looking for a site-distribution which optimizes the station coverage and minimizes the influence of shallow structure and topography of the Earth. In contrast, in volcano-seismology we are left with sometimes very rough topography and nearly unknown propagation and site properties of the medium. Some of these aspects will be discussed in 13.3.

13.1.2 Why use seismology when forecasting volcanic eruptions?

The use of seismological observations in the monitoring and forecasting of volcanic eruptions is justified because nearly all seismically monitored volcanic eruptions have been accompanied by some sort of seismic anomaly. The Pinatubo 1991 (Pinatubo Volcano Observatory Team, 1991) or the Hekla 2000 eruption (http:// hraun.vedur.is/ja/ englishweb/heklanews.html#strain) are two recent examples of successful long- and short-term eruption forecasts made by mainly seismic observations. For further case studies on volcanic "early warning" see the comprehensive articles by McNutt (1996, 2000a, 2000b).

While most of these "early warnings" were simply deduced by counting the number and type of volcanic events per hour or day or even better by monitoring their hypocenter distributions, the physical meaning of the different seismic events and their relationship to the fast ascending magma are not well understood. To give an example: increasing volcanic tremor is always a sign of high volcanic activity, but although the occurrence of tremor will increase the alert level, its role for short-term prediction is still not known precisely enough because we do not know the related physical process of this signal (fluid flow; movement of magma, water and/or gas; crack extension etc.). Further: how can we distinguish between an intrusion and a developing eruption, both of which generate a large number of seismic signals?

The extensive use of seismic methods during the last decades has shown that using them alone will not help the improvement of our knowledge about the internal processes of rapid magma ascent. This will be discussed in more detail in 13.5. Planning a new monitoring network or a short-term seismic experiment, we must also keep in mind that every volcano has its own characteristics, both with respect to seismic signal generation and wave propagation effects.

13.2 Classification and source models of volcano-seismic signals

Most of the confusion in volcano seismology is caused by the huge number of different terms for classifying volcano-seismic events. While this is mainly caused by the imperfect knowledge about the source mechanisms, we will focus on the basic nomenclature widely used in the literature. Most of these terms simply describe the appearance and frequency content of the signal, while others imply a certain source mechanism. However, one should be aware in both cases that the sources are still unknown and the propagation medium may alter the shape and the spectral content of the signals significantly.

While pioneering work in classifying volcano-seismic signals was made by Shimozuru (1972) and Minakami (1974), most of the following discussion follows the work of McNutt (1996, 2000a) and Chouet (1996a). We will divide the known signals mainly into transient and continuous signals. We will also discuss, where appropriate, differences in the signal generation related to different types of magma (i.e., low/high viscous, gas rich/ poor).

13.2.1 Transient volcano-seismic signals

13.2.1.1 Volcanic-Tectonic events (deep and shallow)

Deep (below about 2 km) *Volcanic-Tectonic* events (VT-A) manifest themselves by the clear onsets of P- and S-wave arrivals and their high frequency content (> 5Hz). This leads also to the class name *high-frequency* event (HF) (Fig. 13.1).

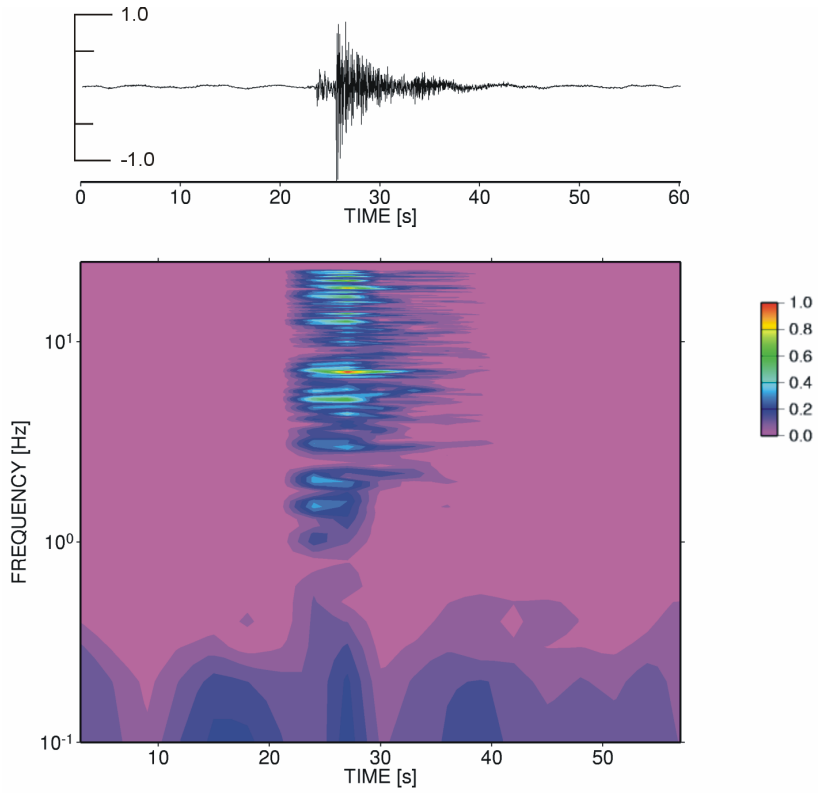

Fig. 13.1 VT-A type event recorded at Mt. Merapi, Indonesia. The impulsive P- and S-wave arrivals are clearly visible in this signal, as well as their high-frequency content and short signal duration. The given color coding, representing normalized amplitude spectral density, is valid for all following figures.

The name of this event type implies a well known source mechanism, namely a common shear failure caused by stress buildup and resulting in slip on a fault plane similar to a tectonic earthquake source. The only difference from the latter is the frequent occurrence of swarms of VT events which do not follow the usual main-after-shock distribution (McNutt, 2000a). An earthquake swarm is a sequence where the largest events are similar in size and not necessarily at the beginning of the sequence. The high frequencies and the impulsiveness of the P- and S-wave arrivals seem to be caused by low scattering due to the short travel path through high scattering regions and low attenuation.

In contrast, *shallow* (above about 1-2 km) *Volcanic-Tectonic* events (VT-B) show much more emergent P-wave onsets and sometimes it is even impossible to detect any clear S-wave arrival (see Fig. 13.2). The spectral bands are shifted to lower frequencies (1-5 Hz). Both observations are thought to be caused by a more shallow hypocenter location and therefore a larger amount of scattering during wave propagation, especially of higher frequencies. While the depth distribution deviates significantly from that of VT-A events, the source mechanism may still consist mainly of a simple double-couple source.

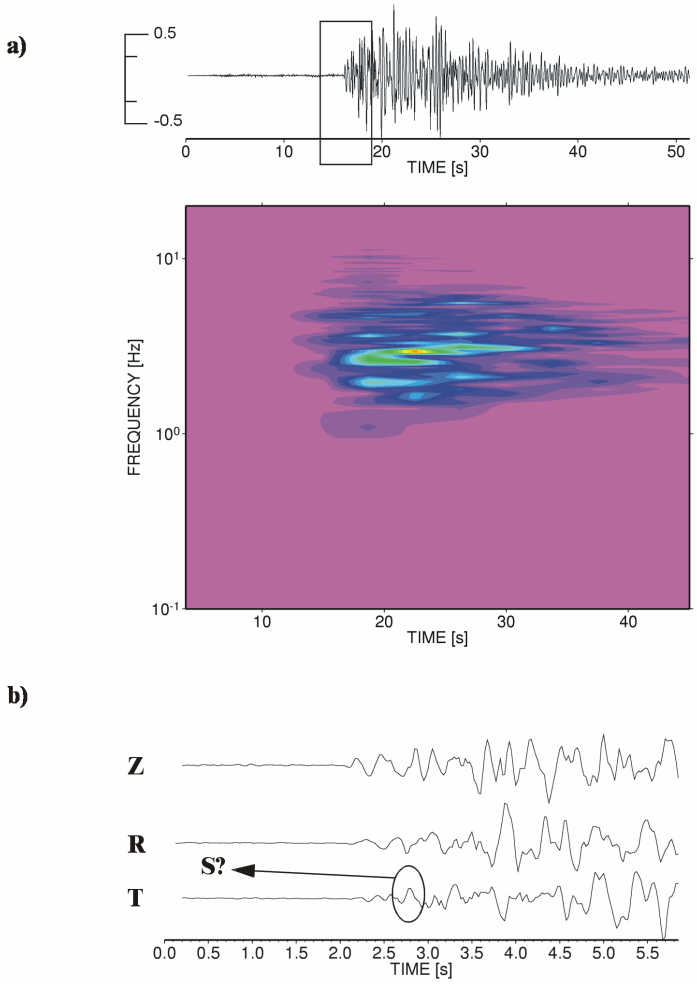

Fig. 13.2 a) typical example of a VT-B type event recorded during a high activity phase at Mt. Merapi. Note that the overall frequency content is mainly between 1 – 10 Hz with a dominant frequency at roughly 3 Hz. b) zoomed out version of the same event in its three components. Whereas the P-wave arrival is clearly visible, no clear S-wave arrival can be seen. The circle marks the wavelet that has the approximate S-wave travel time for the estimated source location.

Recently, detailed studies showed that the sources of some VT events deviate significantly from that of a pure shear failure, but show some similarities with the later described *Low-Frequency* events. Several papers on the inversion of the seismic moment tensor showed a significant contribution of non double-couple parts (Dahm and Brandsdottir, 1997; Saraò et al., 2001).

13.2.1.2 Low-Frequency events

Low-Frequency events (LF or Long Period - LP) show no S-wave arrivals and a very emergent signal onset (see Fig. 13.3). The frequency content is mostly restricted in a narrow band between 1-3 Hz. The LF sources are often situated in the shallow part of the volcano (< 2 km). Locations are deduced mainly by amplitude distance curves, from the rare hypocentral determinations using clear first onset recordings, and recently by semblance location techniques from particle motions recorded on a broad-band seismometer network (Kawakatsu et al., 2000). Some volcanoes (e.g., Kilauea) are known to produce deep (30-40 km) LF events (Aki and Koyanagi, 1981; Shaw and Chouet, 1991).

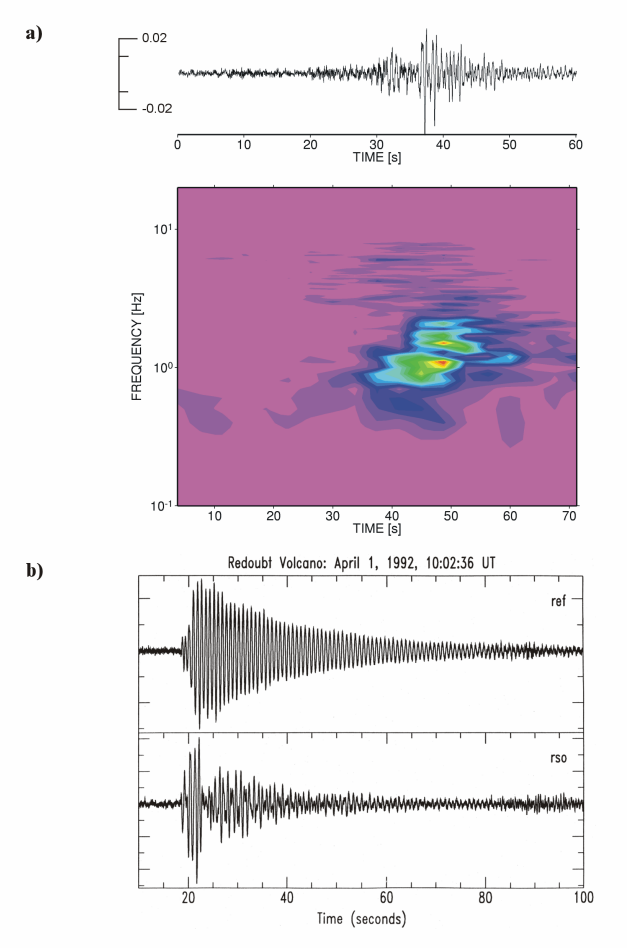

Fig. 13.3 a) example of a LF-wave group recorded at Mt. Merapi. Clearly the dominant frequency is around 1 Hz. b) shows an example of a LF event recorded at two different sites located at Redoubt volcano, Alaska (courtesy of S. McNutt, Alaska Volcano Observatory; AVO). The spindle shaped signal is also known as Tornillo.

The associated source models range from an opening and resonating crack when the magma is ascending towards the surface (Chouet, 1996a) to existence of pressure transients within the fluid-gas mixture causing resonance phenomena within the magma itself (Seidl et al., 1981). Both models are able to explain a large part of the observed features in the spectral domain. Recently a pure crack model was developed which also considers the influence of the fluid properties. Recent numerical simulations show that the resonance effect and the overall shape of the seismograms and their frequency content may also be explained by fluid-solid contact and the excitation of multiple reflected borehole waves (Neuberg et al., 2000).

13.2.1.3 Hybrid events, Multi-Phases events

Some volcano-seismic signals share the signal and frequency characteristics of both LF and VT-(A,B) events. Signals of this class are usually labeled as *Hybrid events*, which may reflect a possible mixture of source mechanisms from both event types (see Fig. 13.4). For example, a VT microearthquake may trigger a nearby LP event. Lahr et al. (1994) and Miller et al. (1998) detected swarms of *Hybrid events* during the high activity phase of Redoubt (Alaska) and Soufriere Hills volcano (Montserrat, West Indies), respectively. Miller et al. (1998) concluded that such events reflect very shallow activity associated with a growing dome.

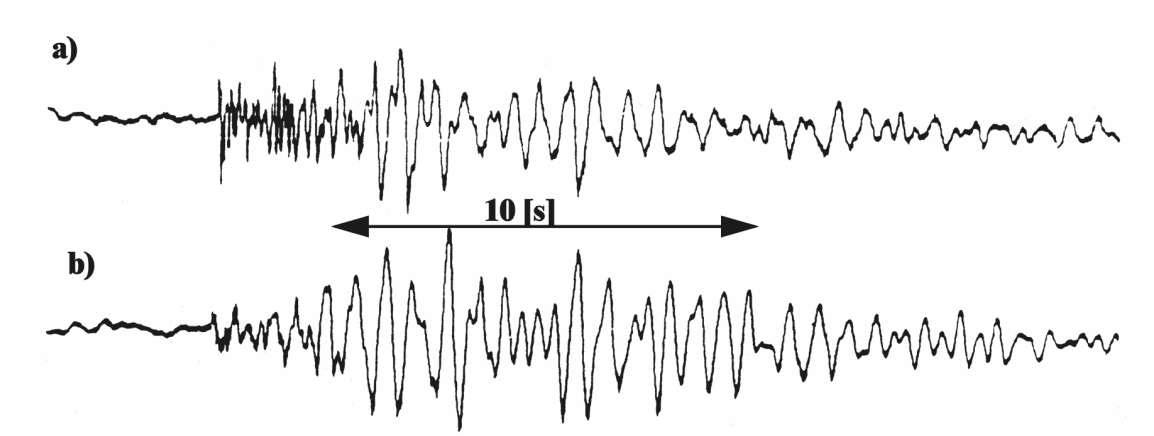

Fig. 13.4 a) shows a Hybrid event and b) a VT-B event for comparison. The higher frequencies at the beginning of the Hybrid event are an obvious feature, while the later part shows the similarity with the VT-B event (courtesy S. McNutt, AVO).

Multi-Phase events (MP also *Many-Phases* event; see Fig. 13.5; Shimozuru, 1972) are somewhat higher in their frequency content (3 to 8 Hz) than *Hybrid* events but are related as well to energetic dome growth at a very shallow level. Both types of signals and their associated mechanisms are still a topic of research as their occurrence might be a good indicator for the instability of high viscous lava domes.

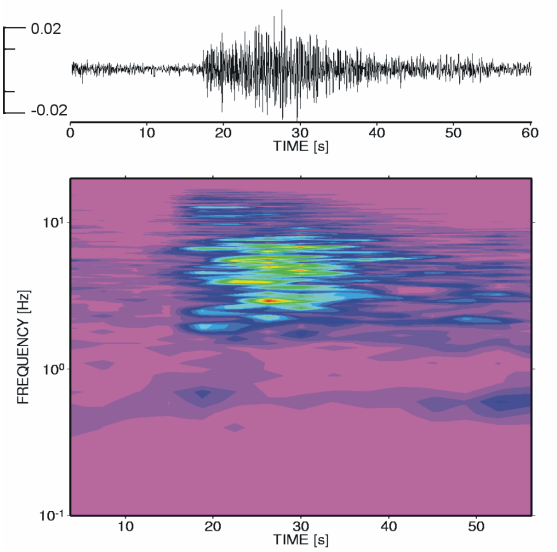

Fig. 13.5 MP-event recorded at Mt. Merapi during strong dome formation. The frequency is restricted between 3 - 10 Hz and resembles that of a VT-B type event at this volcano. Note the long duration of this event whilst its amplitude is much smaller than for the VT-B event shown in Fig. 13.2.

13.2.1.4 Explosion quakes, very-low-frequency events, ultra-low-frequency events

A very pronounced ULP and *very low frequency* (VLF; f ~ 0.1 - 0.01 Hz) signals were made at several volcanoes in Japan and on Hawaii (e.g., Aso: Kawakatsu et al., 2000; Iwate: Nishimura et al., 2000; Kilauea: Ohminato et al., 1998) using several broadband seismometers located in the near-field to intermediate-field distance from the source. Some of class with clear signal characteristics are the *explosion quakes*. This signal class accompanies Strombolian or other (larger) explosive eruptions. Most of these signals can be identified by the occurrence of an air wave which is caused by the sonic boost during an explosion, when the expanding gas is accelerated at the vent exit (see Fig. 13.6). This wave mainly travels through the air with the typical speed of sound (330 m/s). While we do not discuss the explosive mechanism, the source which causes this explosion is not yet clear. Some LF events show the same frequency-time behavior as the explosion quakes but lack an air phase (McNutt, 1986). This might reflect a common source mechanism of deeper situated LF-events and shallow produced explosion quakes.

Portable broadband seismometers with corner frequencies as low as 0.00833 Hz shed new light on this open question (see Fig. 13.7). It could be verified that at Stromboli volcano (Italy) an “ultra-low frequency” (ULF; ultra-long period ULP, f < 0.01 Hz) pressure buildup takes place several minutes before the onset of a Strombolian eruption (Dreier et al., 1994; Neuberg et al., 1994; Wassermann, 1997; Kirchdörfer, 1999). As this is only visible in the near-field of the seismic sources with a geometrical spreading factor proportional to r^{-2}, the seismic stations must be located close to the active vent of the volcano (see Fig. 13.7). A model which fits the visual and seismological observation very well consists of a shallow magma chamber and a tiny feeder system to the surface. The accumulation of a gas pocket and the accent of this pocket as a gas slug may explain the observed pressure buildup (Vergniolle and Jaupart, 1990). However, some of the Strombolian eruptions at Stromboli show no or very small over-pressure (long-period displacement signals) without any visible difference in the associated surface activity.

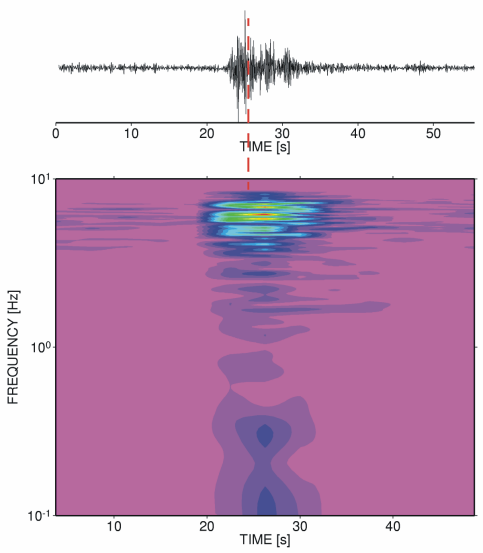

Fig. 13.6 An explosion signal recorded at Stromboli volcano, Italy. The seismic station was located just 400 m from the active vent. The dashed line gives a rough estimate of the onset of a sonic wave also visible as high (red) amplitudes in the time-frequency plot around 5 Hz.

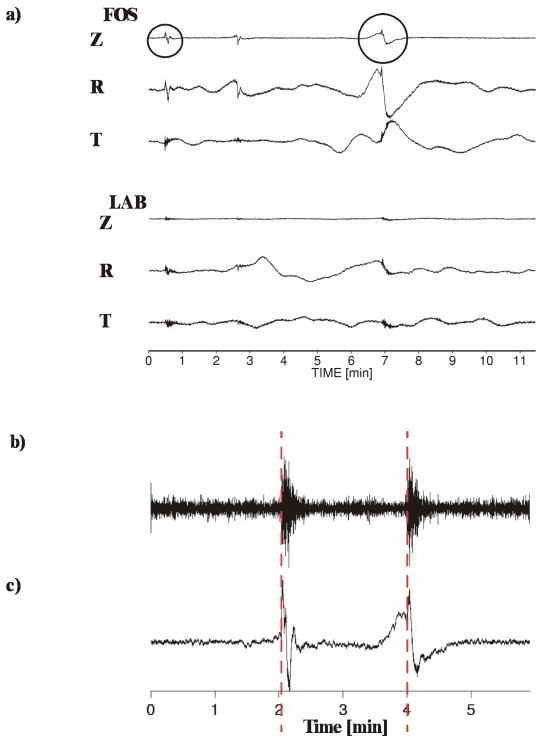

Fig. 13.7 a) ULP signal recorded with a Streckeisen STS2 broadband seismometer (DS 5.1) at Stromboli volcano. We removed the instrument response down to 300 s and the resulting traces are integrated to reflect ground displacement. The three uppermost traces show the three-component seismograms of a station located 400 m from the vent, whereas the lower three traces show the same but at a site located 1800 m from the active vent indicating a large signal only visible in the near-field. b) shows the seismogram of a 1 Hz seismometer during two different explosion quakes, the dashed lines mark the onset of strombolian eruptions. c) shows the displacement signal of two different explosion quakes also visible in a). Note, not all explosion signals are producing the same amount of long-period displacement signals.

Since the late 1980s many of these observations were interpreted as shallow situated (z < 1.5 km) phreatic eruptions with a strong low frequency pressure pulse (f ~ 0.01 Hz; see Fig. 13.8). At the same volcano, Kawakatsu et al. (2000) also detected a second signal with dominant frequencies roughly at 0.06 Hz in the same depth range than the phreatic source. The authors classified this signal as *long period tremor* (LPT) which reflect the merging of isolated pulses into a nearly continuous signal (see Figs. 13.9 and 13.14). Kawakatsu et al. (2000) interpreted the signals as caused by the interaction of hot magma/fluid with an aquifer situated in 1 - 1.5 km depth below the craters of Aso volcano.

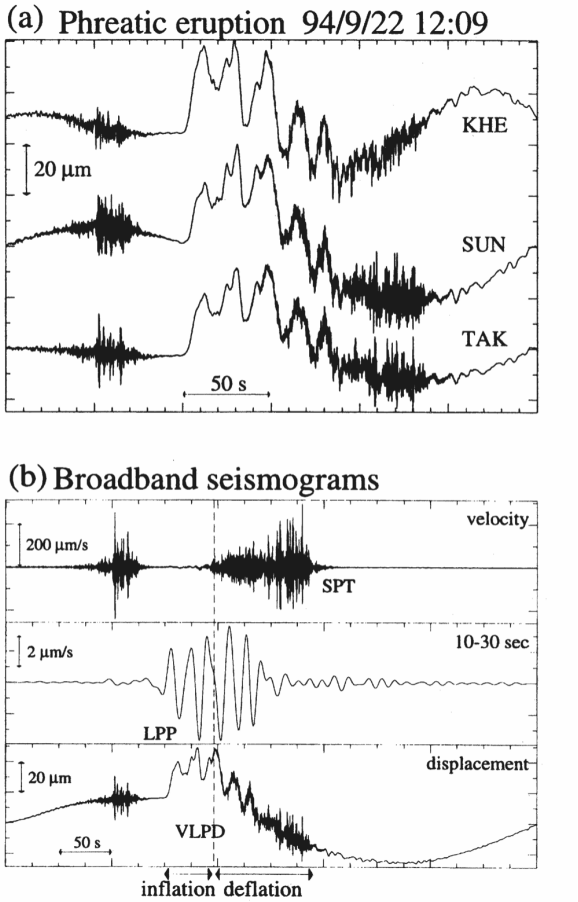

Fig. 13.8 a) ULP (or very long-period displacement) signal observed at three broadband stations during a phreatic eruption of Aso volcano. b) original velocity, band-pass filtered velocity and displacement seismogram of the same event observed at station TAK. The vertical line in b) indicates the onset of the eruption (Kawakatsu et al., 2000).

ULF and VLF events are still unknown at most andesitic and rhyolitic volcanoes, which possibly implies that slug flow (low viscous; Vergniolle and Jaupart, 1990) may be operative. In contrast, the work of Hidayat et al. (2000) showed that there exists a moderate (0.25 Hz) VLF signal in the near-field of some MP events recorded at Mt. Merapi (Indonesia).

In recent years, various approaches were made to investigate the dynamics of the different sources of the VLF and ULF signals using moment tensor analysis. While the estimation of the centroid moment tensor became a standard technique in earthquake seismology (e.g., NEIC and Harvard rapid moment-tensor solutions), the application of this technique in

volcano seismology is restricted to specific applications. The difficulties are manifold. First of all the influence of topography is neglected in the standard approaches, which results in large misfits of the computed synthetic Green's functions. Moreover, Ohminato et al. (1998) showed that even when assuming a horizontal layered medium, the knowledge of the source location and the velocity model with a high confidence is needed in order to apply this technique. Compensated linear vector dipole solutions (CLVD) are often biased by the uncertainty of the assumed simplified velocity structure. However, there are some applications of moment-tensor estimations with VLF and ULF signals which give reliable results, indicating source mechanisms which deviate significantly from a pure double-couple solution commonly known of tectonic earthquake mechanisms (e.g., Fig. 3.10 from Legrand et al., 2000; Ohminato et al., 1998; Aoyama and Takeo, 2001). A further example and more references concerning seismic moment tensor inversion and non double-couple mechanisms of volcanic seismic signals are given in Saraò et al. (2001).

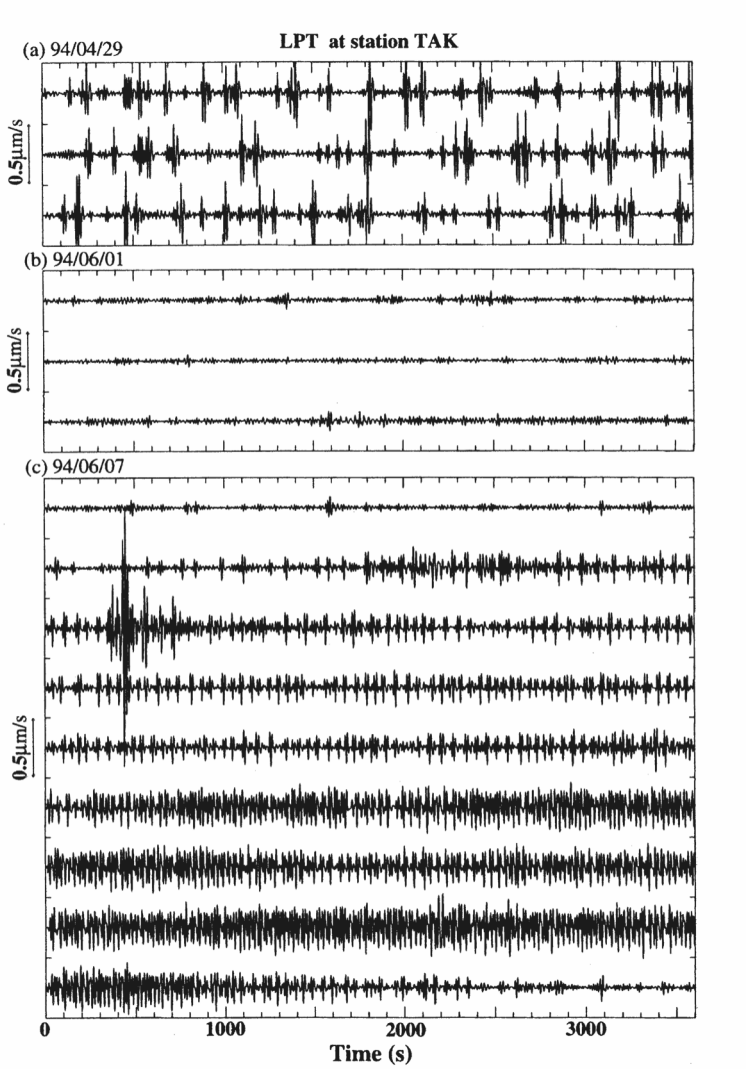

Fig. 13.9 Vertical component broadband seismograms band-pass filtered at 0.033 to 0.1 Hz at Aso volcano during three different days in 1994. The isolated ULP pulses visible in a) and b) were merged together in c) forming the continuous signal of *long period tremor* (Kawakatsu et al., 2000).

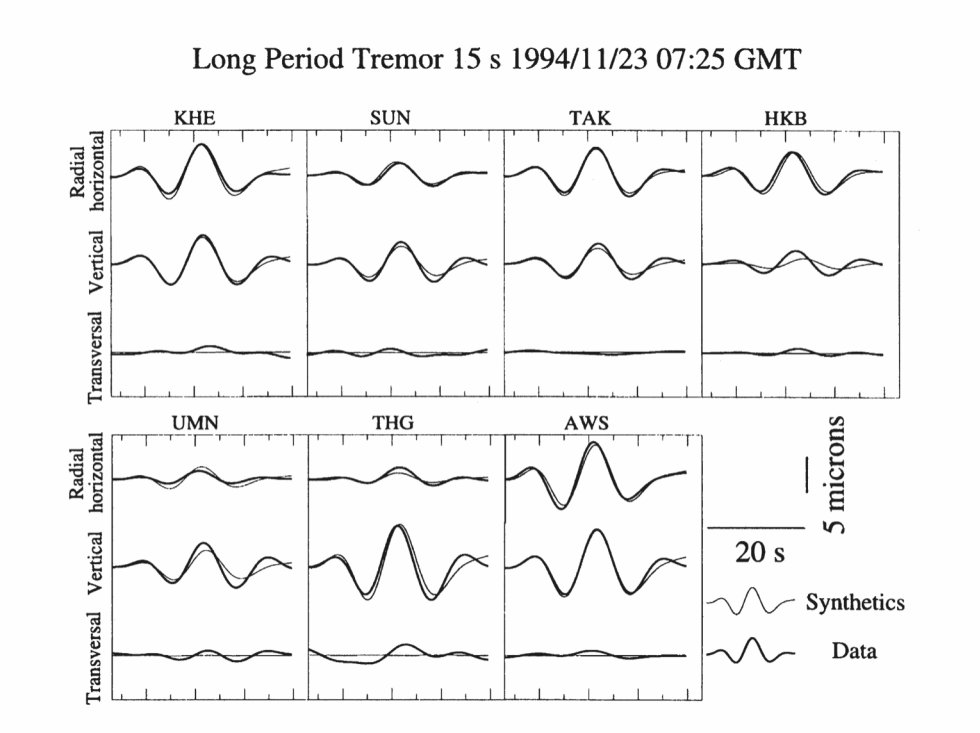

Fig. 13.10 Data (thick) and synthetic (thin) seismograms calculated from an inversion of the seismic moment tensor for a single pulse of *long period tremor* at Aso volcano. The corresponding source mechanism consists of a large isotropic component (97%) in addition to a small deviatoric part (Legrand et al., 2000).

13.2.2 Continuous volcanic-seismic signals

The appearance of continuous seismic signals at active volcanoes demonstrates the most profound difference between tectonic earthquake and volcano seismology. The suspected mechanisms range from obvious surface effects such as rockfalls, landslides or pyroclastic density flows to internal ones such as volcanic tremor. Nearly every volcano world-wide shows the signal of volcanic tremor during different activity stages. Volcanic tremor is the most favored parameter in volcano early eruption warnings. Because of possibly differing source mechanisms, we discuss tremor separately for the two flow regimes: high and low viscosity.

13.2.2.1 Volcanic tremor (low-viscous two-phase flow and eruption tremor)

Most of the monitored basaltic volcanoes show some kind of cyclic appearance of *volcanic tremor*. The tremor signals can last between minutes and months in duration and, in most of the cases, their spectra are very narrow-band (1-5 Hz; Fig. 13.11). Some tremor signals show strong and short-pulsed amplitude variations (termed *beating tremor*), while others are nearly stationary over several days or even months. The common similarities in the spectra of volcanic tremor and LF and even explosion quake events is another important observation which has to be explained when looking for the source mechanisms. At Mt. Etna volcano (Italy), strong fluctuations of volcanic tremor amplitude are associated with lava fountaining at one of its summit craters or after the opening of a flank fissure (Cosentino et al., 1989).

Gottschämmer (1999) described a tremor cycle at Bromo volcano (Indonesia) where the tremor amplitude fluctuation could be correlated with heavy ash plume (large amplitude - *eruption tremor*) or white steam (small tremor amplitude) episodes (see Fig. 13.11).

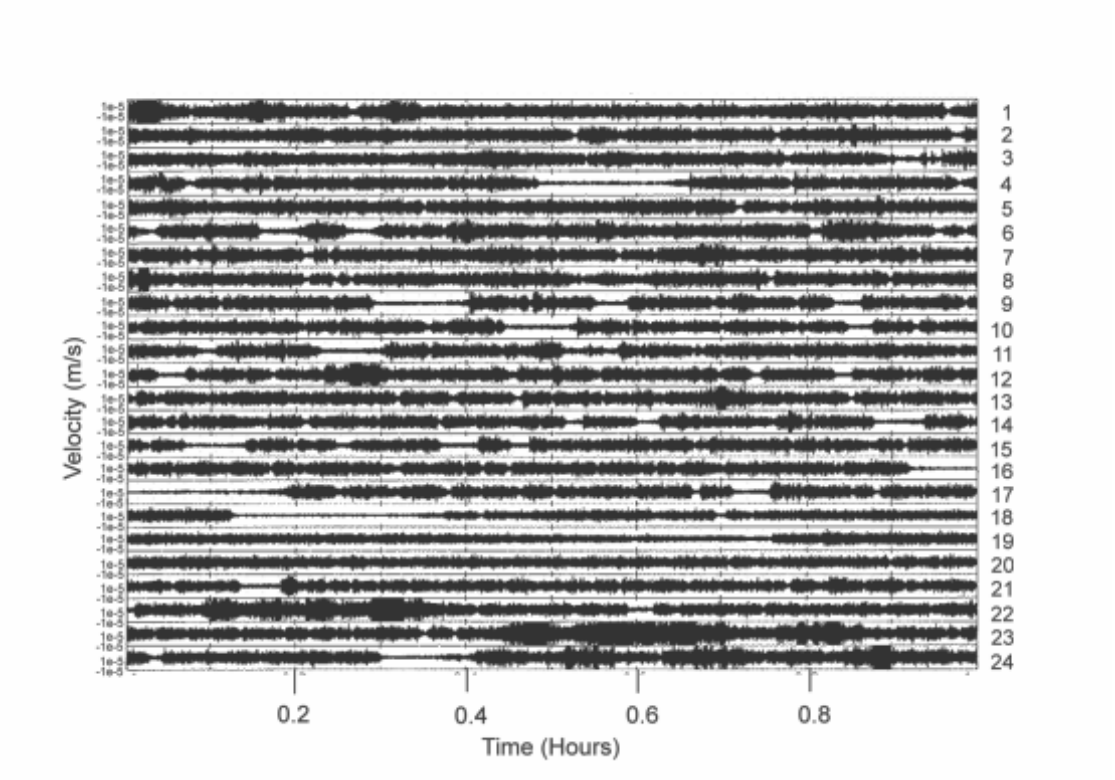

Fig. 13.11 Volcanic tremor at Bromo volcano (Indonesia) during a high activity phase at the end of 1995 (courtesy of E. Gottschämmer, University of Karlsruhe). Large tremor amplitudes correlate with the eruption of heavy ash plumes while small tremor amplitudes appear during quiet steam emissions (Gottschämmer, 1999).

These observations made at different volcanoes with either low viscosity magma or a huge amount of volatiles (free or after the fragmentation of high viscosity magma; steam) suggest the involvement of gas/fluid interaction in generation of volcanic tremor. The similarities in the overall spectral content of LF events and volcanic tremor is reflected in similarities of the proposed source mechanism or of the source region (resonating fluid). Flow instability is thought to play an important role in the excitation of volcanic tremor in multiple phase flow pattern (Seidl et al., 1981; Schick, 1988) and the associated LF events are seen as a transient within the same physical system. On the other hand, Chouet (1986) and Chouet (1987) state that a repeated excitation of a connected crack system could cause a harmonic and long-lasting signal, where the fluid is only passively reacting to the crack oscillations.

The spectral content observations support both the low viscosity magma and volatile interpretations. Explosions at Stromboli volcano excite the same frequency band as does volcanic tremor, which supports the idea of a common resonating system (see Fig. 13.12). However, care must be taken when interpreting the frequency spectra of volcanic tremor. Detailed studies on the spatial frequency distributions at Stomboli showed that single frequency peaks are possibly influenced, to an unknown amount, by the propagation medium (Mohnen and Schick, 1996).

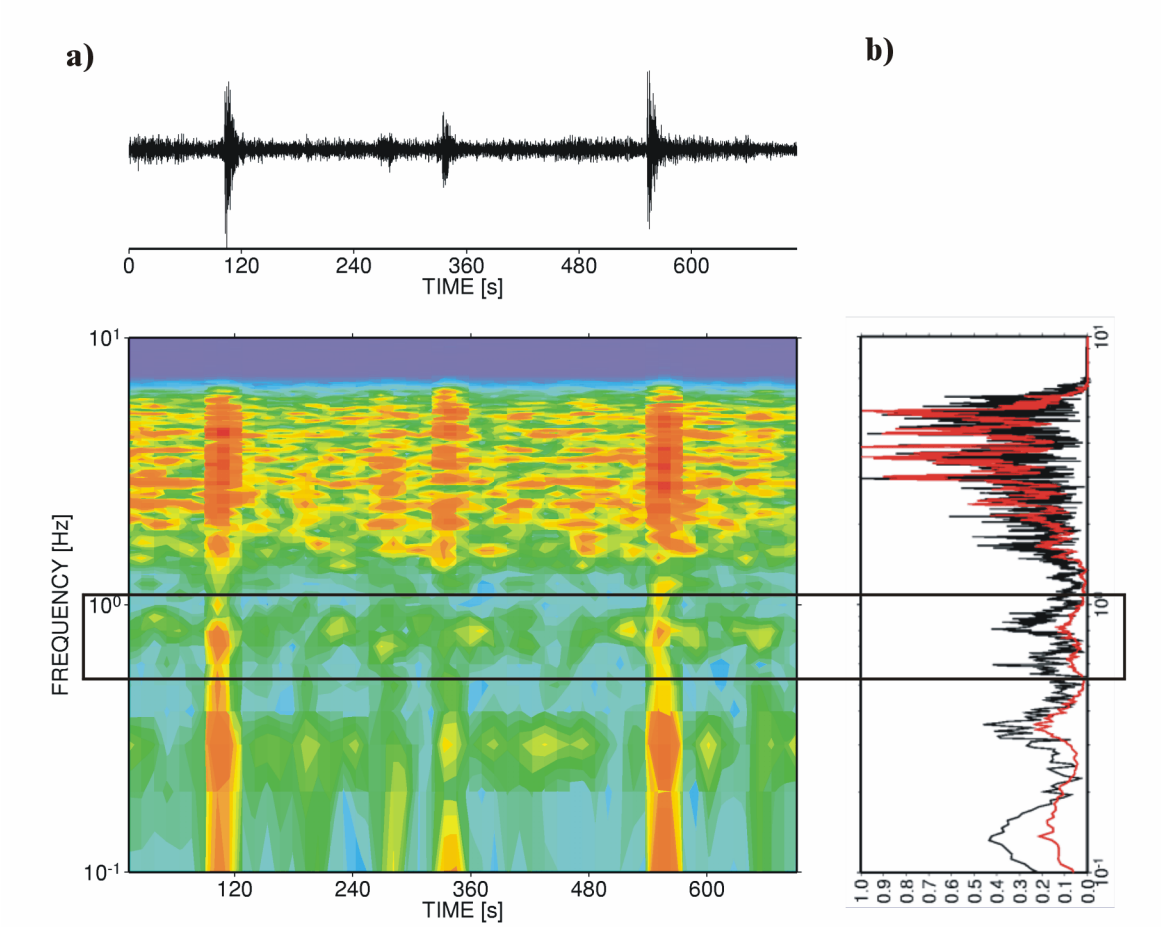

Fig. 13.12 a) explosion signals superimposed on the continuous signal of volcanic tremor at Stromboli volcano. The box marks the frequency band of weak but typical volcanic tremor band at Stromboli volcano. Note that the explosion quake also excites the same frequency band whereas below this frequency band the spectral amplitude of the explosion quake type signals are somewhat smaller. The tremor band with frequencies above 2.0 Hz is partially distorted by the ejected volcanic debris falling back to the surface and tumbling down the slope of the volcanic edifice (see 13.2.2.3). b) the normalized Fourier transform of an explosion quake type signal (black) and of a noramilzed power spectrum of six hour continuous recording (red). While the first reflects the typical spectrum of all explosion quakes, the overall behavior of the second spectrum is mainly due to volcanic tremor. The overall similarity between the explosion quake and tremor signal types is obvious.

13.2.2.2 Volcanic tremor (high-viscous - resonating gas phase)

During the last decade, many observations were made of the occurrence and characteristics of volcanic tremor at volcanoes with high-viscosity lava. At Semeru volcano (Indonesia) the spectra of volcanic tremor contained up to 12 overtones. This supports the assumption of a resonating medium with a high quality factor (Q) as well as a precisely working feedback mechanism (Hellweg et al., 1994; Schlindwein et al., 1995) (see Fig. 13.13). Similar observations were also made at Lascar volcano (Chile), where up to 30 overtones could be identified in the seismic signals (Hellweg, 1999).

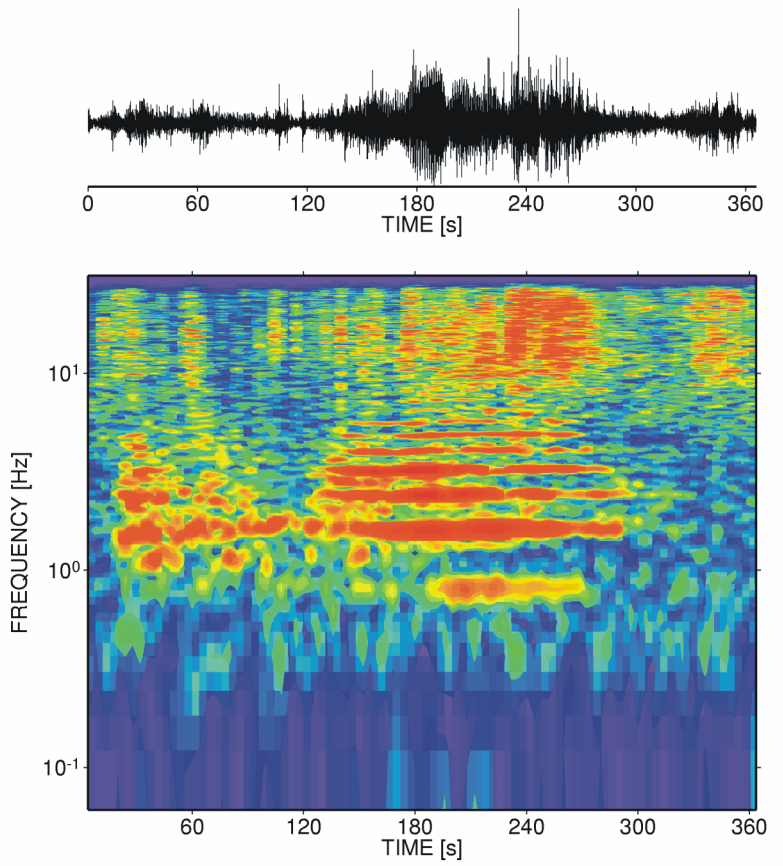

Fig. 13.13 Harmonic tremor signal recorded at Mt. Semeru, Indonesia. Up to six overtones can be recognized starting with a fundamental mode located at roughly 0.8 Hz.

Schlindwein et al. (1995) proposed a feedback mechanism similar to that of sound generation in a recorder, and also discussed a repeating source with precise repetition time as a possible mechanism. This model was refined by Johnson and Lees (2000) and Neuberg et al. (2000). In the feedback mechanism case, the resonating body must consist of a pure gas phase, but the lava at Mt. Semeru is too viscous for resonating at the observed frequencies. The second mechanism requires a very precise timing mechanism for producing the highly stable overtones.

Recent observations at Montserrat volcano (Neuberg et al., 2000) and Mt. Merapi volcano (Indonesia) support the hypothesis of a repeating source (see Fig. 13.14). During several cycles of increased volcano-seismic activity we recognized the transition from closely timed MP/Hybrid events into the continuous signal of volcanic tremor and vice versa. As the source mechanisms of both types of signals are still unknown, the driving force behind these mechanisms is not known. Also the type of feedback mechanism which must be involved in this system could not yet be identified.

Volcanic tremor, as previously noted, is always a sign of high activity. However, since the exact mechanisms are still unknown, the importance and timing between the first appearance of tremor and possible eruptive activity is still a matter of discussion (McNutt, 2000a).

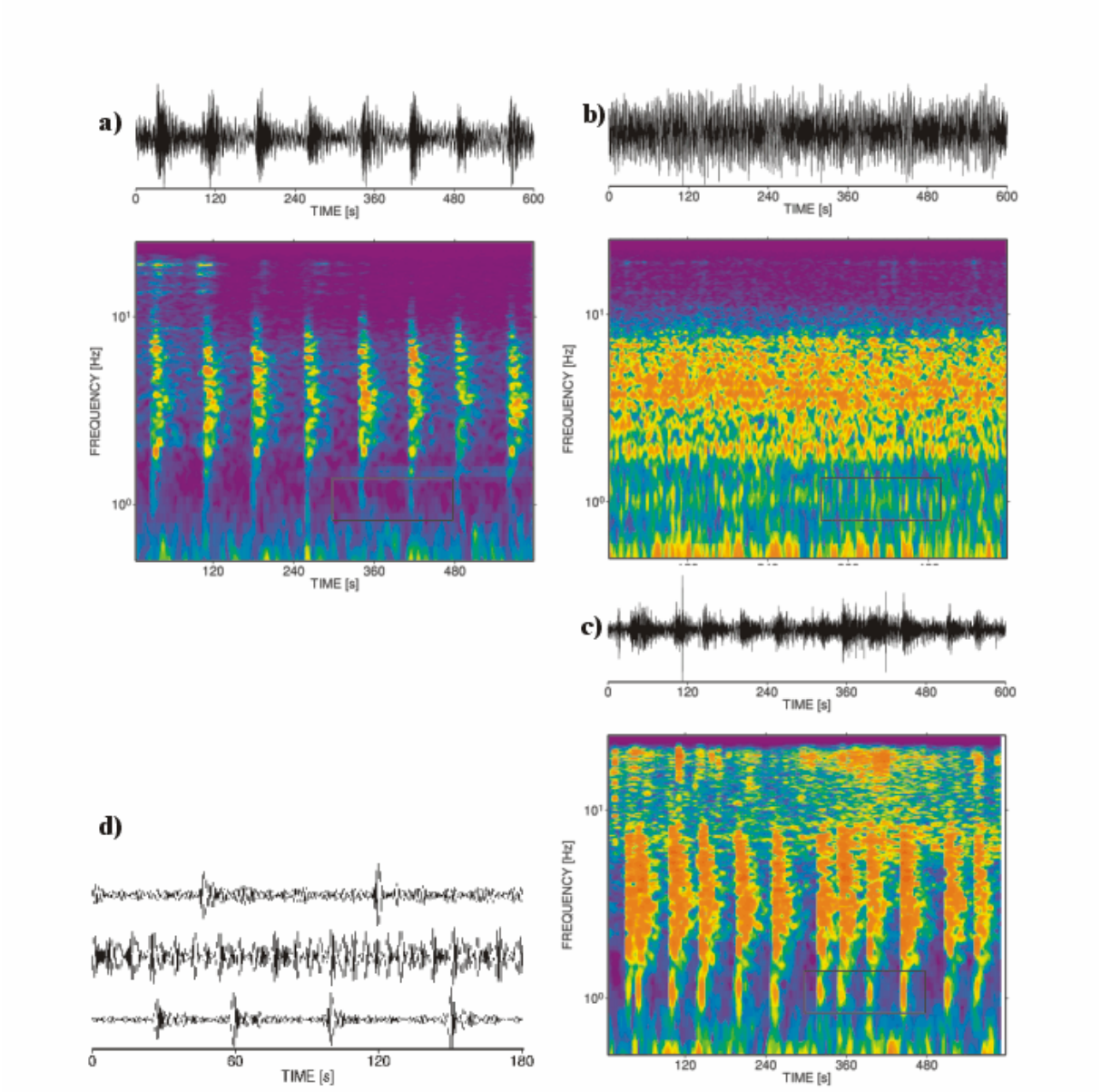

Fig. 13.14 Sequence of repeated seismic signals at Mt. Merapi volcano in 1996: a) very regularly timed MP-events before they merge together to form volcanic tremor (see b); c) after some hours the tremor is replaced by a sequence of discrete events with slightly higher amplitudes than before. Note: in contrast to the classification given in Fig. 13.5, the frequency content of these signals is lower (0.7 - 10 Hz) and might not resemble "pure" MP-events. In d) the time-frequency region of plots a)-c) are plotted in time domain. A band-pass between 0.8 - 1.3 Hz was applied before zooming. The individual wavegroups seen in the filtered continuous signal also supports the idea of the merged events causing the volcanic tremor.

13.2.2.3 Surface processes

Substantial release of seismic energy at active volcanoes is related to surface processes acting directly on the volcanoes edifice. For example, pyroclastic flows, lahars (volcanic debris flows) and rockfalls from unstable domes or crater walls can generate seismic signals with

amplitudes exceeding several times those of the typical volcano-seismic signals. The most important signals for monitoring purposes are those associated with pyroclastic flows and lahars. The monitoring of lahars, which includes also acoustic and visual monitoring, is especially important when monitoring a volcano which is capped by a glacier or which is located in a tropical area. Melting of the snow during an eruption or heavy rainfall during rainy season will occasionally mobilize a huge amount of volcanic debris. The signals of all this activity are mostly high-frequency (>5 Hz) and show spindle (cigar) shaped seismogram envelopes that can last several minutes (see Fig. 13.15). The complex waveforms of pyroclastic flows are caused by a mixture of initial collapse of big lava-blocks onto the surface and ongoing fragmentations when traveling down the slope of the volcano (Uhira et al., 1994). During the January/February 2001 eruption of Mt. Merapi, it was also possible to recognize that the very first part of the signal was somewhat lower in frequency (1 - 2 Hz), indicating a possible explosion at the start of the pyroclastic flow (Ratdomopurbo, pers. communication; see also Fig. 13.12). An important monitoring question is: which signal is caused by a rockfall and which by a pyroclastic flow? The low frequency start (1 - 2 Hz at Mt. Merapi) of the latter might be crucial for discriminating between both types of events. This observation made at Mt. Merapi and also Unzen volcano (Uhira et al., 1994) might be used at other volcanoes with an active lava dome as the mechanism of flow generation seems to be the same.

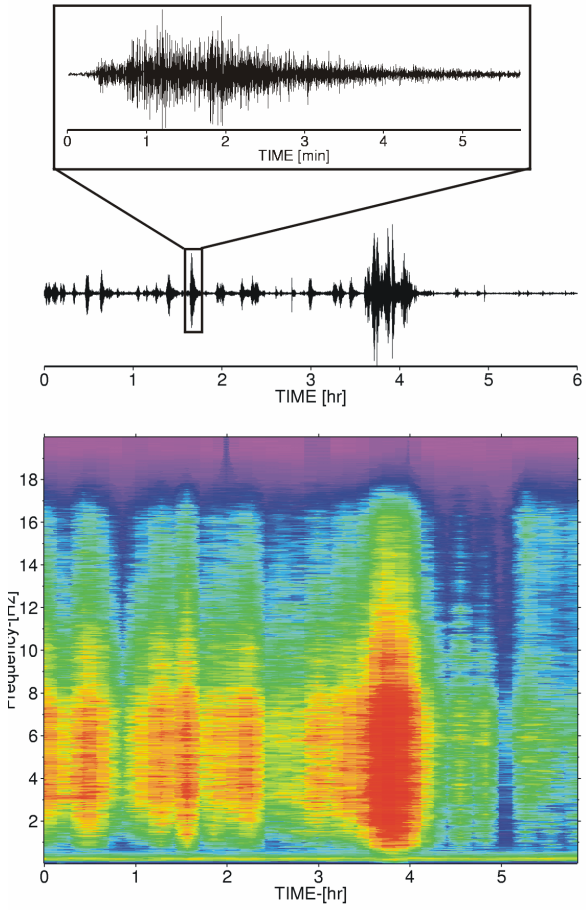

Fig. 13.15 Sequence of medium to larger pyroclastic flows recorded at Mt. Merapi volcano during the 1998 dome collapse. Note the 6-hour time scale and that individual events last many minutes longer than the seismograms of typical earthquakes. Just before 4 hours the largest pyroclastic flow in the whole eruption sequence takes place and lasts for about 30 minutes.

13.2.3 Special note on noise

Most of the extensively monitored volcanoes lie in densely populated areas with much human activity (that is why they are monitored). Hence, care must be taken when interpreting signals usually classified as volcanic tremor. In some cases, human activity excites signals occupying the narrow spectral band between 1-4 Hz (big machines etc.). Also a distinct 24 h rhythm is very likely caused by increasing human activity during daylight time and should therefore be analyzed with special care (see Fig. 13.16). Even when using three-component seismometers it is not easy to discriminate for sure between volcano-seismic and man-made noise. The topography at active volcanoes is very often radially shaped and the propagation paths to the seismic stations are shared by ambient seismic noise and volcanic signals.

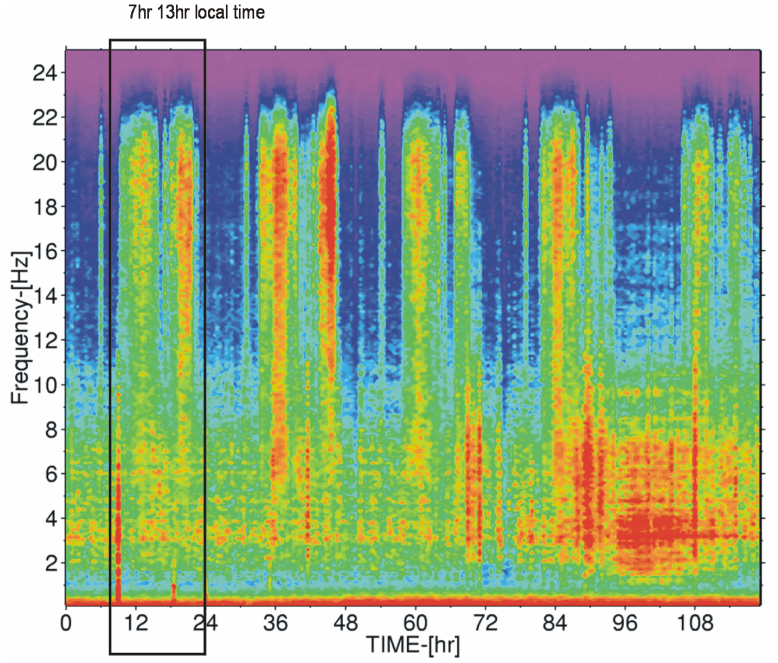

Fig. 13.16 Spectrogram of background noise recorded at a seismic station at Mt. Merapi. As the station is located in farming area, the human daylight activity can be clearly recognized by its distinct 24 hour periodicity. Furthermore, it is possible to see that there are two main working hours during daytime (marked by a box). Large spectral amplitudes are visible around 7 hours local time and a second peak is located around 15 hours hours after a time of quiescence during noon.

In conclusion, we note that most of the above classifications and proposed source mechanisms are deduced from simple observations of spectral content and overall shape of the associated seismograms rather than by physically verified constraints. Care must be taken when interpreting the occurrence of one of these signals during increasing volcanic activity. There are many examples of increasing numbers of VT events and increasing volcanic tremor amplitude without any surface activity at volcanoes. Thus, to be truly effective and diagnostic, seismic monitoring should be complemented, to the extent possible, by other instrumental monitoring techniques (e.g., geodetic, geochemical) and visual observations made regularly of the volcanoes being monitored remotely (see 13.5).

13.3 Design of a monitoring network

One of the most important decisions to be made, when establishing a seismic monitoring network, is the design of the station distribution. In most cases, volcanoes are monitored with at least four to six seismic stations which are distributed around the volcanic center. Newer deployments try to set up arrays of sensors or, even better, a network of different arrays. However, some of the design criteria deviate from the usual earthquake monitoring networks and are discussed in the following sections.

13.3.1 Station site selection

Considering a location as a possible site for a seismic station is always a compromise between noise considerations and accessibility. Of course, it would be best to place the seismic station far away from any human activity (see Fig. 13.16), away from big trees or sharp cliffs and ridges. However, the accessibility is very important, especially at the beginning of a surveillance campaign at a volcano. Also, the rough and harsh environment typical of many volcanoes usually requires frequent station visits for maintenance. Valleys, which generally are accessible places for seismic stations rather than ridges or cliffs, are often flooded during winter or the rainy season (not to mention the higher exposure to possible pyroclastic flows).

A second important decision must be made when choosing on “what” the station should be placed. Usually, seismologists prefer hard rock to unconsolidated sediments. At many active volcanoes, hard-rock sites are rare and, even if they exist, they are not necessarily good choices. Hard-rock sites often are small lava tongues or big blocks of lava buried in ash or soil, causing waveguide effects or even block rotation to an unknown degree. This is especially important when installing broadband seismic stations, which are very sensitive to tilt (see Chapter 5). A network-wide homogeneous installation with good temperature isolation is preferable to apparent “hard-rock” installations (see 13.6 for a more detailed description). Sites near singular obstacles should be avoided such as high trees, cliffs, big towers etc., as they are likely sources of wind-generated noise. While wind noise is usually high in a frequency range > 5 Hz, wind pressure is a very strong source of tilt-noise in the low frequency part (< 0.1 Hz). Hence, special care must be taken when installing a broadband seismic instrument.

13.3.2 Station distribution

Good station coverage is crucial for nearly all monitoring efforts as well as for successful scientific research. A good choice is to install a network at two scales - one large scale network extending into non volcanic regions (Δ < 20 km) and one network with stations concentrated on the flanks and on the top of the volcano (Δ ~ 0 - 2 km). The large-scale seismic networks are very useful to distinguish between volcano-seismic signals and regional or local earthquake activity. Also, the larger dimension improves the localization accuracy for deep-seated sources of magmatic activity. On the other hand, most of the seismic signals at active volcanoes are very shallow and usually small in amplitude. For detailed studies of the volcano-induced seismic signals, most of the stations must be placed close to the activity center(s). One or two stations should be placed as near as possible (without danger to

researchers and instruments) to the active volcanic region. Other stations should be placed so as to ensure a good overall azimuthal coverage. If possible, the station spacing should be comparable to the source depth to insure good depth control. It is good to have all parts of the focal sphere surrounding a source to be sampled by seismic stations. Best results are expected when the source is located within the station network, both lateral and vertical.

If a broadband seismometer is available, best results are achieved if it is installed as close as possible to the active area, provided that the safety of operating personnel is assured. Most of the recorded ULF signals at volcanoes are detectable only in the near-field distance range (see Fig. 13.7). If an on-line radio link is desired, the station site must be chosen so as to guarantee an undisturbed direct line-of-sight to repeaters or receivers (see 13.6 and 7.3).

13.3.3 Seismic arrays in volcano monitoring

Modern approaches to volcano seismology are based on deploying seismic antennas (arrays) at active volcanic areas. Stations in an array should be spaced close enough to sample a wavefield several times in a wavelength, often requiring a spacing of about 100 m. The main advantage of such antennas and the application of array techniques is the improvement in evaluating the radiated wavefield properties, velocity structure and the source location (see Chapter 9). A comprehensive review paper dealing with standard seismic array techniques at volcanoes has been published by Chouet (1996b).

Most of the problems in operating a seismic array at an active volcano are of a technical nature. The requirements on array site conditions are demanding, the cost of array components are rather high, and the installation and maintenance of an array during different activity stages and weather conditions require significant economic and human resources. Such requirements generally preclude the long-term use of arrays in volcano monitoring. Therefore, most of the work done so far in using array techniques at active volcanoes were short-term deployments of occasionally large arrays. Despite the mostly short duration of deployment, however, much information was gathered during these experiments. The results range from a more comprehensive description of the wavefield properties (Saccorotti et al., 1998; Chouet et al., 1997) to tracking the source volume of volcanic tremor signals (Almendros et al., 1997; Furumoto et al., 1990).

13.3.4 Network of seismic arrays

In attempting to achieve both monitoring and research objectives, a good compromise is to establish a network of small-aperture seismic arrays. The advantage compared to single (dense) array applications is the better spatial evaluation of the wavefield properties as well as the better azimuthal coverage when focusing on the location of the different seismic signals. In any event one has to compromise between aperture, number of instruments, spatial sampling and station accessibility. In 1997, a network of small-aperture arrays was established at the Merapi volcano, Indonesia (see Fig. 13.17). This network consists of three different array sites distributed around the volcano. The main objective of this array configuration is to attempt the automatic classification of the volcano-seismic events on the basis of the wavefield properties and an automatic hypocenter determination of the classified volcano-seismic events (Wassermann and Ohrnberger, 2001).

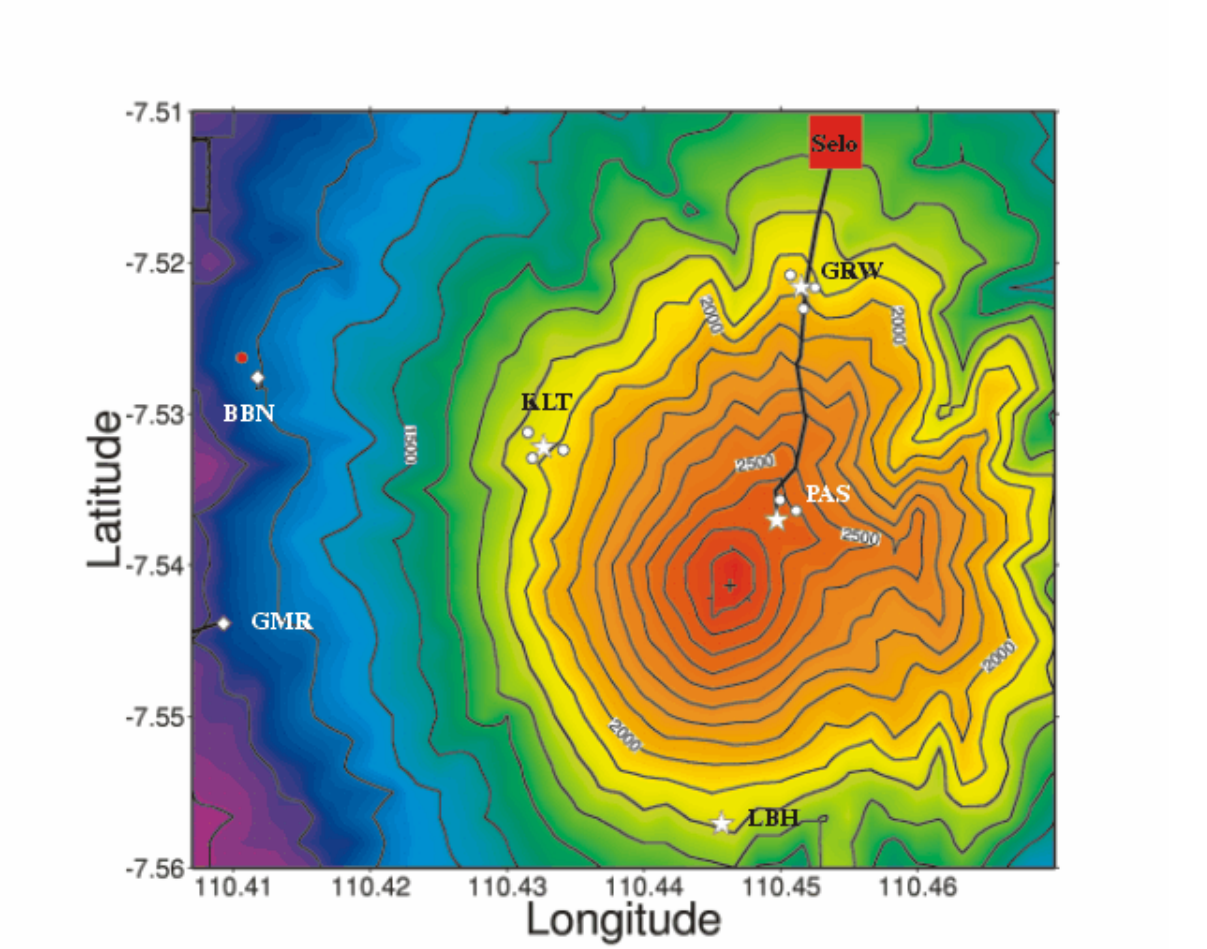

Fig. 13.17 Example of a combined seismic array/network approach at Mt. Merapi volcano. The stars show the location of broadband seismometers, whereas the circles mark the position of three-component short-period seismometers, in total forming three small-aperture arrays. The diamond symbols show the location of seismic acoustic stations (short-period sensors with a microphone array). *LBH* station is not yet installed.

Before installing a network of arrays, a detailed plan should be made of features to be investigated and criteria to be met, e.g., required spatial coverage and resolution, accuracy of hypocenter determination, shallow and/or deep seismicity, broadband signals etc. A good choice will be a network with at least four different array sites. Each array should consist of one three-component broadband seismometer as central station surrounded by three to six short-period, vertical-component seismometers deployed in a configuration which best fits to the number of seismic stations (see Chapter 9). The most suitable distance between related seismometers must be carefully evaluated during the initial stage of the setup. Decisions must be made between the peak values in the spectral domain and the desired coherence band of the signals recorded. Ideally, the stations should be roughly 100 to 200 m apart from each other (see Fig. 13.18). Reducing the inter-station distances with the same number of seismometers will cause an undesired loss of resolution in slowness due to the smaller aperture and also increase the noise coherence (see Fig. 13.18).

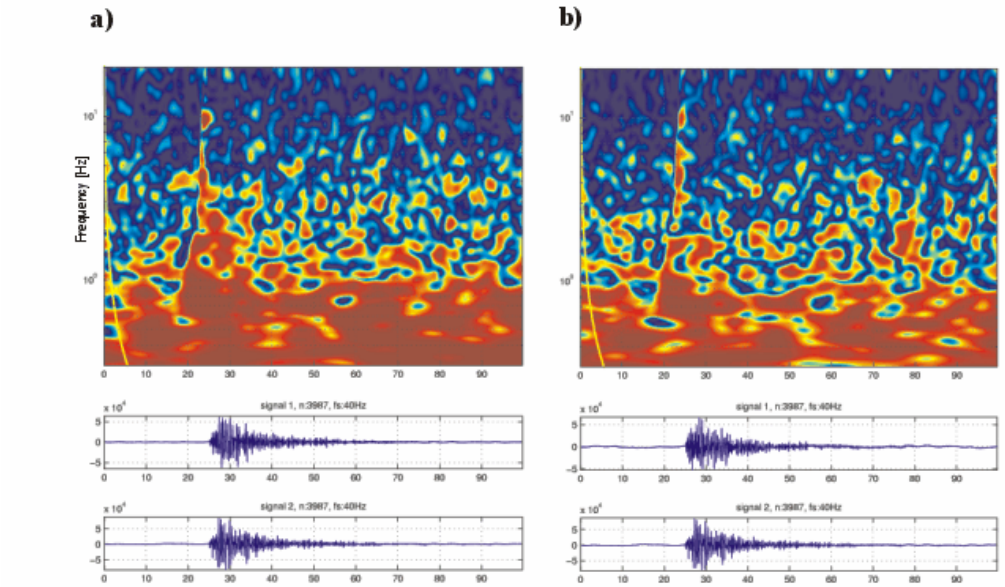

Fig. 13.18 Time-frequency coherence plot of: a) the station combinations GRW0- GRW1; and b) GRW1-GRW2 (see Fig. 13.17). The seismometers in a) are deployed in 170 m distance from each other, whereas in b) GRW1 and GRW2 are separated by roughly 300 m. Note: the signal coherence is computed in a sliding window with the time axis centered at the middle of the sliding window. High coherence above 2 Hz is only visible in the very beginning of a seismic event, indicating an array wide coherent phase arrival. It is also obvious that the overall coherence is somewhat lower in b) than in a) indicating the reduced signal coherence at more separated stations. On the other hand, the noise coherence is also reduced in b) which improves the signal-to-noise ratio of the semblance estimation significantly.

13.4 Analysis and interpretation

Here, we will briefly review the basic techniques of analyzing volcano-seismic signals. Most of the described concepts are based simply on visual pattern recognition abilities of the responsible interpreter. More recent and objective approaches that attempt to automate these tasks are discussed at the end.

13.4.1 One-component single station

Most of the observations made in the 1960s and 1970s were obtained by using only a few instruments located at the most active volcanoes. Since then, nearly all well-monitored volcanoes are equipped with at least four to six instruments and, for a number of volcanoes, dozens of instruments. However, the basics of the classification scheme discussed in 13.2 is deduced by the single station approach and even today the statement “better one than nothing” holds as regards the number of instruments. This is especially true when initiating short-term projects or monitoring very remote volcanoes.

13.4.1.1 Spectral analysis

With the advent of inexpensive, portable and efficient computers, spectral analysis has become an increasingly important tool for monitoring the activity of an active volcano. As mentioned already in 13.2, most of the classification is based on the time-frequency characteristics of seismic signals. Volcanic tremor episodes are distinguished by their spectral shape and appearance. There are many different techniques for computing the spectral seismic amplitude such as *Seismic Spectral Amplitude Measurement* (SSAM; Rogers and Stephens, 1991), short-term Fourier transform or power spectral density estimates, which provide the observer with signal information in the spectral domain (e.g., Qian and Chen, 1996). An important feature of volcano-seismic signals are their narrow-band spectra. In particular, volcanic tremor sometimes shows just one dominant spectral band with a bandwidth as small as 0.2 Hz. This is the reason why it is often called "harmonic tremor". Monitoring the changes of spectral properties is a useful tool not only for signal discrimination but also for characterizing the state of volcanic activity. An example is given in Fig. 13.19. In Fig. 13.19a the total power in the frequency range between 0.6 and 3.0 Hz is plotted as a function of time. This frequency range has been chosen because of its importance in discriminating between rockfall and pyroclastic flow signals (see 13.2.2.3). Three pronounced peaks are obvious with amplitudes well above the average value. The peaks at day 9 and day 18 are associated also with significant increase of the power density between 2 to 10 Hz (Fig. 13.19b). On the other hand, the sharp peak in day 14 in Fig. 13.19a seems to be of a different nature and might be caused by a regional or teleseismic earthquake. The remaining times with high power density amplitudes in b) might be due to small pyroclastic flows or rockfalls.

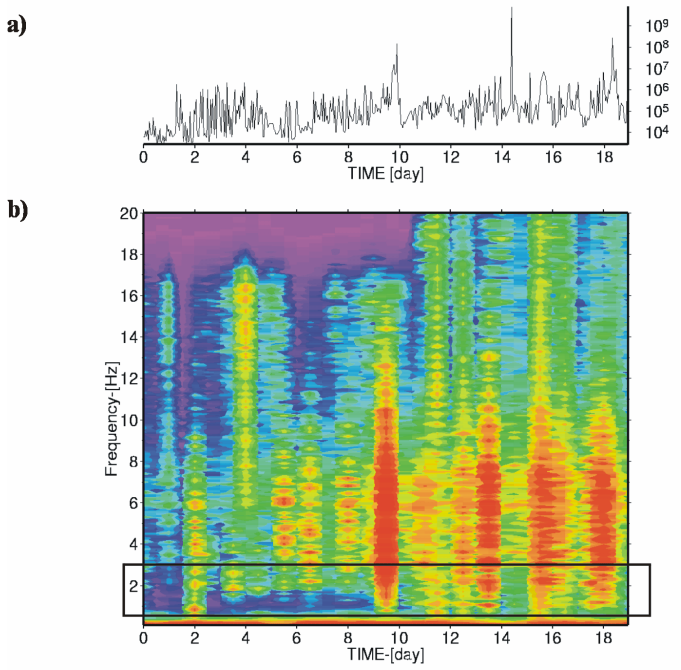

Fig. 13.19 a) shows the the total power (per 60 minutes) calculated in the frequency band between 0.6 - 3.0 Hz from 01 - 19th July 1998 at Mt. Merapi, displayed on a logarithmic scale. Two of the visible peaks (i.e., day 9 and day 18) are associated with pyroclastic flows, while the sharp peak visible at day 14 is caused by a regional earthquake; b) the power spectral density vs. time in the same time range, where the box shows the frequencies used for total power plotted in a).

At Mt. Etna (Italy), Cosentino et al. (1989) reported a significant frequency shift in the volcanic tremor spectra prior to a flank fissure eruption. The authors detected a significant shift to lower frequency values of the dominant spectral peaks of volcanic tremor just several hours before the opening of flank fissures.

Because the efficiency of today's computers is rapidly increasing, a good choice would be to calculate complete spectrograms (or periodograms) first and decimate the amount of data only in a later step (e.g., to SSAM). This would allow the extraction of any hidden information in a later "off-line" step of the analysis without any redundant work load. Crucial in this context is a good knowledge of the possible features of different signals and their relationship to the state of volcanic activity at a specific site. It must be emphasized that stations of monitoring networks at volcanoes should be maintained for years (even decades) without any changes in the system (gain, position etc.). When upgrading an old station with "up-to-date" technology, a sufficient overlap of both systems should be guaranteed. This precaution can not be overemphasized.

13.4.1.2 Envelope, RSAM and cumulative amplitude measurements

An added important source of information which can be deduced by small networks is the overall appearance of the signal shape in the time domain. This is important both for event classification (e.g., volcanic tremor, rockfall etc.) as well as for monitoring changes in the seismic activity of a volcano. A very efficient tool for visualizing increasing seismic activity is the *Real-Time Seismic Amplitude Measurement* (RSAM) technique proposed by Endo and Murray (1991). In its original form, RSAM was designed for analog telemetry and consisted of an A/D converter, averaging of the seismic signal in 1 min or 10 min intervals and storing of the reduced data on the computer:

$$RSAM(iT) = \frac{1}{T} \sum_{t = iT - \frac{T}{2}}^{iT + \frac{T}{2}} |s(t)|$$

With T as the averaging interval (originally 1 or 10 min) and $s(t)$ the sampled seismic trace. Various examples for successful applications of this technique are given by McNutt (2000b).

Some applications try to normalize the records from several seismic sensors located in different distances from the volcanic center by correcting the measured seismic amplitude for the assumed source distance (McNutt, 2000b):

$$D^b{}_R = \frac{Ar}{2\sqrt{2}G}, \text{ and } D^s{}_R = \frac{A\sqrt{\lambda r}}{2\sqrt{2}G}$$

where D^b and D^s are the reduced amplitude for body and surface waves, respectively. A is the peak to peak amplitude in centimeters, r the distance to the source, λ the seismic wavelength in cm and G the gain factor (magnification) of the seismic sensor. The only difference between these two equations are the different correction terms for the geometrical spreading. The reduced amplitude measurements should be considered as a pure observation parameter without any physical meaning. It should definitely not be used for the physical interpretation

of an ongoing eruption. The reduction of the seismic amplitude assumes specific modes of wave propagation, i.e., body waves and surface waves, respectively. As there is no reliable estimation of the wavefield properties, it is possible with just one or a few seismometers that the assumption of the degree of geometrical spreading is highly speculative. Also, the effect of site amplification and the strong scattering observed frequently at volcanoes (Wegler and Lühr, 2001), which depend in general on the source location, structure and topography of the volcano, may alter the amplitude-distance relationship significantly. They are neglected in this approach.

Another way of displaying changes in the radiated seismic wavefield is based on the computation of the de-trended cumulative radiated power of the seismograms at a single station (see Fig. 13.20):

$$P_{cum}(f_{1-2}, t) = \sum_{t} \left(\sum_{f=f_1}^{f_2} P_t(f) - trend \right)$$

with $P_t(t)$ being the power spectral density during time interval t and f_1, f_2 the upper and lower frequency for computing the cumulative power. *trend* is the slope of the cumulative power, calculated during a quiet, i.e., baseline activity of the volcano (see Fig. 13.20).

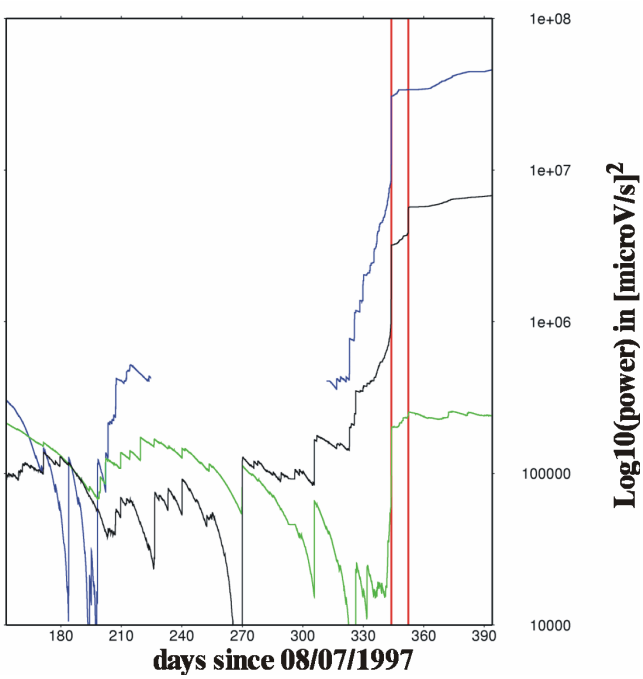

Fig. 13.20 De-trended cumulative power of the vertical components of all broadband seismometers at Mt. Merapi during 1998 activity. The red lines mark the occurrence of two pyroclastic flows. A steep increase of the total cumulative power 10 days before the onset of the first pyroclastic flow is visible, following a period with very low seismicity. Also the second eruption is preceded by an increase of cumulative power at two stations, while one station (blue) was out of operation. The background trend was estimated during a low activity phase in 1997.

To avoid a fast saturation of the cumulative power values, a good way is to estimate the slope of the cumulative power when the activity of the volcano is on its baseline. This estimated trend can be removed for each time step resulting in a de-trended cumulative power plot, which shows strong deviation from the "normal" background seismicity. Furthermore, cumulative power can analyze certain frequency bands (see Fig. 13.19a), unlike the power change in time which resembles the method of RSAM. In Fig. 13.20, the de-trended cumulative power of three broadband stations at Mt. Merapi is shown. Note the steep increase of seismic power roughly ten days prior to the first eruption. A further increase in cumulative power is obvious for two stations preceding the second large pyroclastic flow. The third station was out of operation caused by ash fall on the solar panels.

A common way to display information on the current status of a volcano is to count the different seismic event types in a hourly or daily manner (see Fig. 13.21). While the interpretation of the type of an event is sometimes impossible or an intuitive judgment when using only one station, such event/time plots are an excellent tool for displaying all information (objective and subjective) within one single plot. There are many papers which rely strongly on this kind of activity measurements. Most of the observations are summarized by McNutt (1996, 2000b). Also in this case, we must emphasize that, without a complementary detailed seismological study, this is just a visualization of observed patterns with, strictly speaking, unknown physical meaning.

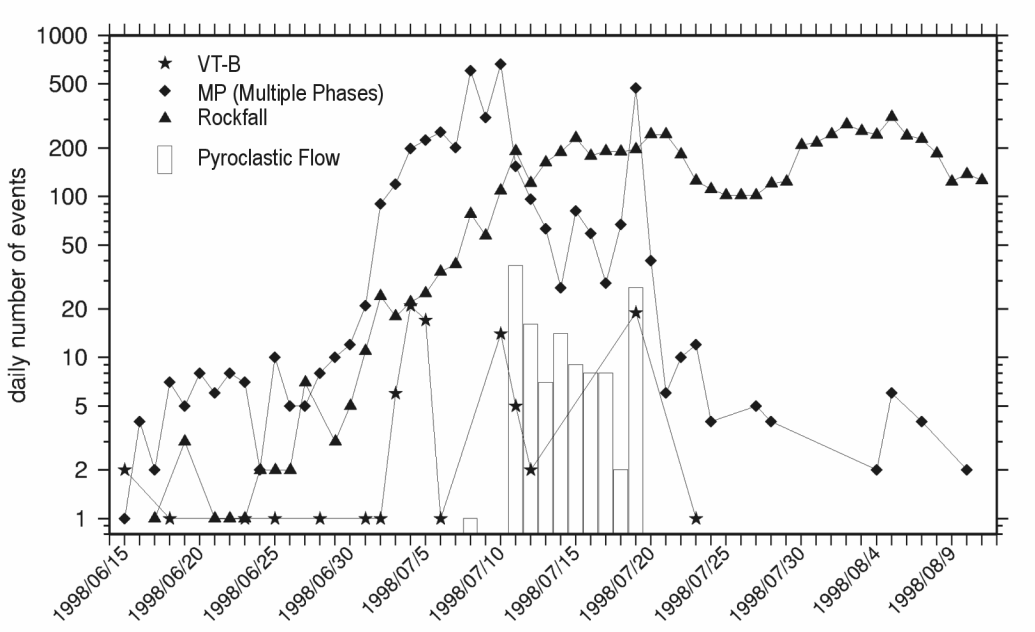

Fig. 13.21 Event-type per day plot during the high activity of Mt. Merapi during July 1998. Note the increase of the three event classes before the onset of the first pyroclastic flow. Also note the similarity of the VT-B type event curve to the occurrence of pyroclastic flows (courtesy of VSI- BPPTK, Yogyakarta).

On the other hand if knowledge about the hypocenters (see 13.4.3.1) and even source mechanism is available these event-time plots are very valuable in order to evaluate the activity state of a volcano. At Soufriere Hills volcano (Montserrat Island) it was possible to distinguish different activity phases with the help of these seismicity plots (Miller et al., 1998). Just before the surface activity starts to develop, a swarm of VT-A earthquakes

appeared. During cycles of inflation in the upper part of the growing dome a large number of Hybrid and LP events were detected. Finally, a large number of surface events, mainly rockfall signals, were recorded when the dome was getting more and more unstable. While these patterns of seismic signals are very important during a high activity phase of a volcano, it must be emphasized that every volcano and every eruption has its own unique pattern.

13.4.2 Three-component single station

Most modern seismometers are three-component sensors which record the vector of ground motion produced by seismic waves. Observation of the particle motion will not help to precisely determine source locations and their variations without a detailed knowledge of the wavefield properties (e.g., Rayleigh waves, Love waves, P or SH and SV waves). Changing patterns of particle motion may help estimate the activity changes of a volcanic system in a qualitative way, however.

13.4.2.1 Polarization

Seidl and Hellweg (1991) showed results from analyzing the 3D-trajectories of a single seismic broadband station at the Mt. Etna volcano (Italy) using very narrow bandpass filters. They argued that the occasional strong variations in the azimuth and incidence angles of the trajectories might reflect sudden changes of the active source location. Recent experiments using array techniques, however, showed that the wavefield radiated from a volcanic source is a combination of complex source mechanisms and strong path influences (e.g., Chouet et al., 1997). Hence, the wavefield consists of a mixture of many wave types and care must be taken when only polarization information is available. On the other hand, carefully extracted information and the associated changes of polarization pattern during different cycles of volcanic activity may help to identify changes in the state of the volcanic system (see Fig. 13.22 below).

The use of a broadband seismic station located close to an active vent, i.e., in the near-field, improves the quality of source estimations based on simple polarization analysis. This is because of the small influence of the propagation path in the near-field. Unfortunately, complicated source mechanisms, i.e., when the usual assumption of a point source is no longer valid, will complicate the interpretation of the observed polarization pattern to an unknown degree (Neuberg and Pointer, 2000). Also, the nearly unknown influence of the topography of the volcano on signals with a wavelength comparable to the topographic obstacle will make interpretation difficult. Recent near-field measurements at Stromboli volcano (Italy) showed that, in some cases, a fairly good estimation of the source region could be made using just a single three-component broadband station (Kirchdörfer, 1999; Hidayat et al., 2000) under the assumption of a simple source mechanism.

13.4.2.2 Polarization filters

When evaluating the polarization properties of volcano-seismic signals as part of a monitoring system, an automatic estimation of parameters is needed. Best results will be obtained when focusing on the basic parameters, i.e., the azimuth, incidence angle and a measure of the rectilinearity of the signals. Various approaches will extract this information from a

continuous data stream. Most of them are based on a least-square fit of the 3D-trajectory of the seismic vector to a 3D-ellipsoid. Typical algorithms consist of solving the eigenequation and simultaneously searching for the orientation of the eigenvector corresponding to the largest eigenvalue (e.g., Flinn, 1965, Montalbetti and Kanasewich, 1970):

$$\begin{bmatrix} x_i \\ y_i \\ z_i \end{bmatrix} \left[\underline{C} - \lambda_i \underline{I} \right] = 0$$

where x_i, y_i, z_i represent the components of the i-th eigenvector, $\underline{I}$ is the identity matrix and λ_1 is the eigenvalue according to the i-th eigenvector. $\underline{C}$ represents the covariance matrix of the 3D signal recorded:

$$C_{ij} = \sum (u_i - \bar{u}_i)(u_j - \bar{u}_j)$$

where u_i, u_j are the i-th and j-th component of the seismic sensor and $\bar{u}_i$, $\bar{u}_j$ represent the mean values of the data traces within the analyzed time window. A possible way to display the polarization properties vs. time is to plot the orientation of the eigenvector associated with the largest eigenvalue (corresponding to the major axis of the ellipsiod) in the coordinate system of the sensor, i.e., its azimuth Φ_{az} and incidence angle Θ_{inc}:

$$\Phi_{az}(t) = \text{atan}\left(\frac{y_1(t)}{x_1(t)}\right), \text{ and } \Theta_{inc}(t) = \text{atan}\left(\frac{z_1(t)}{\sqrt{x_1^2(t) + y_1^2(t)}}\right)$$

with x_1, y_1, z_1 representing the eigenvector components of the largest eigenvalue $\lambda_1(>\lambda_2>\lambda_3)$. Note: without any further assumption of the analyzed wave-type, i.e., P, SH or SV wave etc., the computed azimuth has an ambiguity of 180 degrees, whereas the incidence angle varies between 0 - 90 degrees. Typically, a measure of the rectilinearity of the signal's polarization (i.e., the relative elongation of the ellipsoid in one direction) is computed (e.g., Vidale, 1986):

$$L(t) = 1 - \left(\frac{\lambda_2(t) + \lambda_3(t)}{\lambda_1(t)}\right)$$

L(t) is only larger than 0 if λ_1 is bigger than the combination of the other two. Fig. 13.22 gives an example of the variation of the parameters Φ_{az} and Θ_{inc} over a long time range at Stromboli volcano.

Because we have no knowledge of the wave type represented by the computed polarization parameters, they must be seen as varying activity parameters rather than interpreting them as part of a technique for hypocenter determination.

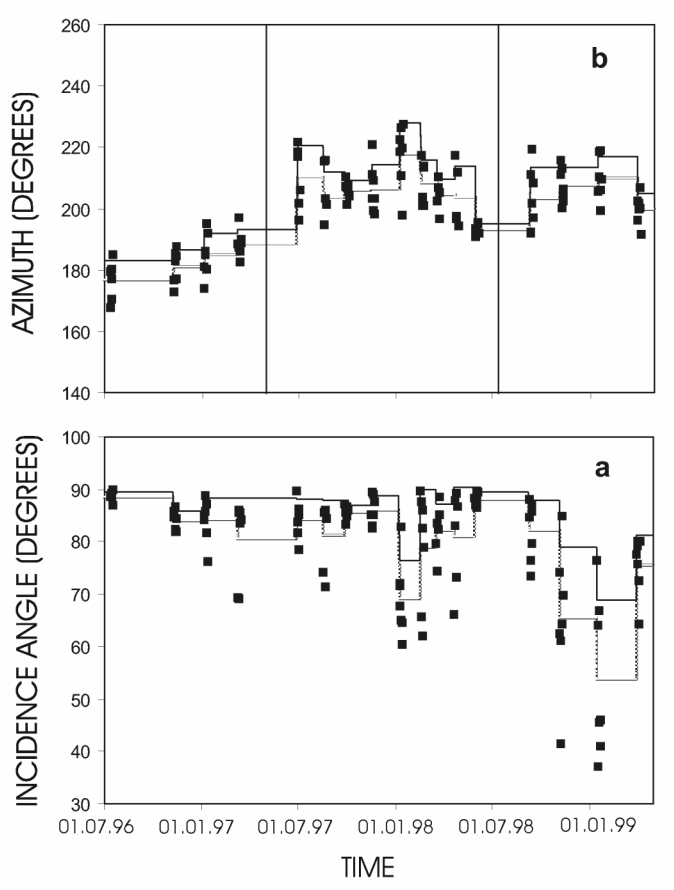

Fig. 13.22 Long-term variations of incidence angle (a) and azimuth (b) in the 115 time windows selected from July 1996 to April 1999 at Stromboli volcano. In both panels, solid and dotted lines depict mean value and standard deviation, respectively, computed over 5 to 7 consecutive days in the 17 time windows selected from July 1996 to April 1999. The polarization parameters were estimated using the technique of Montalbetti and Kanasewich (1970). The variation of this waveform information seems to match changes in the activity states of the volcano (courtesy of S. Falsaperla, Istituto Nazionale di Geofisica e Vulcanologia).

13.4.3 Network

13.4.3.1 Hypocenter determination by travel-time differences

Modern seismic monitoring networks at active volcanoes usually consist of at least four to six seismic sensors distributed in various azimuths and distances from the volcanic center. While continuous signals, such as volcanic tremor or transients like LF-events, often lack any clear phase arrival, some signals (VT, explosion quake) with clear onsets can be located using standard seismological techniques.

Usually, events with clear P- and/or S-wave onsets are selected visually and the first breaks are picked interactively. The inversion for the source location is frequently done using algorithms such as HYPO71 (Lee and Lahr, 1975) or HYPOELLIPSE (Lahr, 1989). Note, however, that most of the standard hypocenter determination programs are based on the assumption of a horizontally layered half-space and/or models with linear gradients with no

topography. Also new approaches exist, which are not restricted to 1D or 2D velocity models and which try to locate the sources in a non-linear, probability based manner (e.g., Lomax et al., 2000). However, in most cases no good velocity models for the monitored volcanoes exist, and the computed source coordinates, especially when focusing on shallow events, must be seen just as an approximation of the true hypocenter. Relative earthquake locations of multiplets with similar waveforms can greatly improve the resolution of volcanic structures (Rubin et al, 1998; Waldhauser and Ellsworth, 2000; Ratdomopurbo and Poupinet, 1995).

There are many papers on the topic of imaging the hypocenter distribution during or before a volcanic eruption (e.g., Newhall and Punongbayan, 1996; Power et al., 1994; Chouet et al., 1994). Very useful information about the geometry of the plumbing system as well as the physical properties of the host rocks can be deduced by analyzing the time-space pattern of frequently occurring swarms of deeper earthquakes (Power et al., 1994).

Also the migration of hypocenters during a high activity phase of a volcano is important in forecasting the following volcanic eruption. In Fig. 13.23, an example of the 1991 Mt. Pinatubo eruption is shown. The migration of the seismic events from a cluster at 5 km depth north-west of the volcano in A) to a very shallow location directly underneath the erupting vent in B) is very obvious and possibly marks the ascending magma.

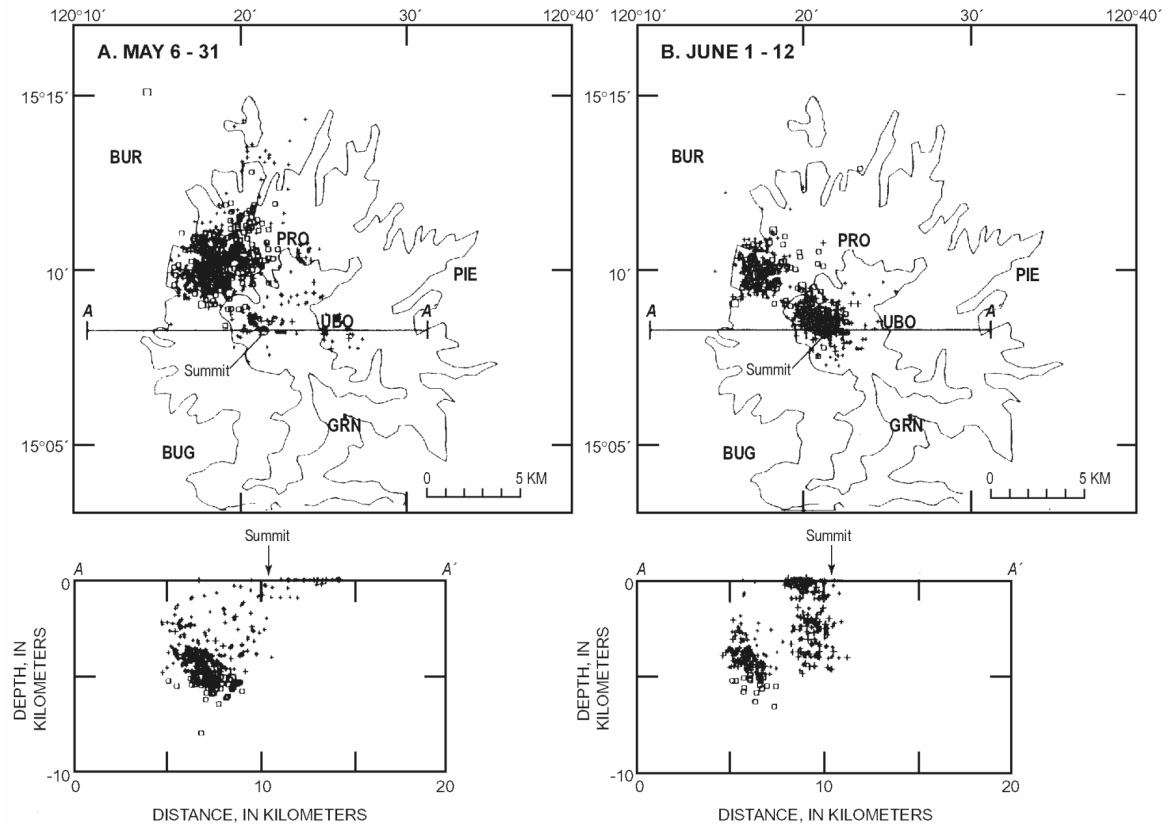

Fig. 13.23 A) Mt. Pinatubo seismicity during May 6 to May 31. The seismic events are clearly clustering northwest of the volcanic center. B) shows the seismicity between June 1 to June 12 indicating a shift of the hypocenters to shallow depths and closer to the summit of Mt. Pinatubo (courtesy of Pinatubo Observatory Team (1991), EOS Trans. Am. Geophys Union, 72, 545, 552-553, 555).

13.4.3.2 Amplitude - distance curves

Even in the case of no clear P- or S-wave arrival, it is sometimes possible to estimate an approximate source area. Assuming a certain wave type (body or surface wave), neglecting an uneven radiation pattern of the source, and assuming a simplified propagation path, it is possible to compute amplitude-distance curves and model the source region. This can be seen as an iterative approach of fitting or contouring the amplitudes or radiated energy measured in the whole network. Successful applications of this technique were reported for locating volcanic tremor at Bromo volcano, Indonesia (Gottschämmer and Surono, 2000) and Mt. Etna, Italy (Cosentino et al., 1984). However, care must be taken in the *a priori* assumption of the wave-type, i.e., body or surface waves. Wegler and Lühr (2001) showed that the largest amplitudes visible in the seismograms recorded at the Mt. Merapi volcano are fitted best by assuming a strong scattering regime, which also alters the amplitude-distance relationship. Also the influence of near-field effects may influence the amplitude-distance curve significantly (see Fig. 13.24).

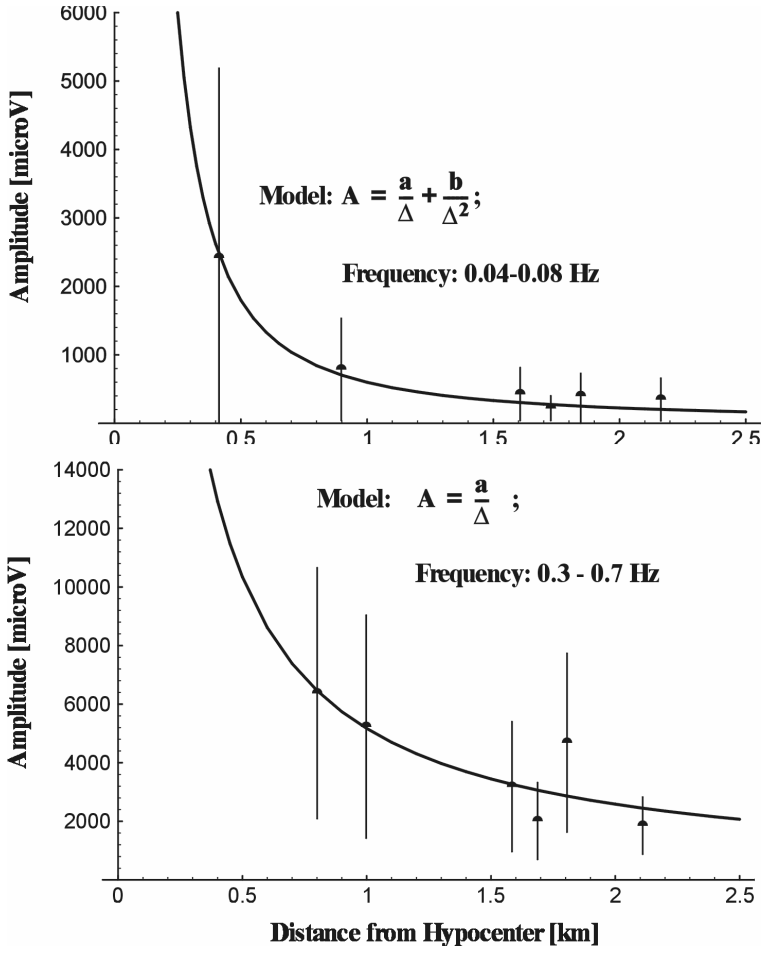

Fig. 13.24 Upper diagram: amplitude-distance relationship at Stromboli volcano; the amplitudes were measured in the frequency range 0.04 - 0.08 Hz. The best fit of the amplitudes at different distances from the active vent was obtained when an additional near-field term was added ($A \sim 1/\Delta^2$). Lower diagram: same as above but in the frequency range 0.3 - 0.7 Hz. In this case, the best fitting curve follows the usual factor of geometrical spreading $1/\Delta$ for body waves. It is also obvious that in b) site effects are more pronounced than in a).

13.4.4 Seismic arrays

The analysis of seismic signals using array techniques is seen as the most prominent and emerging modern tool for locating volcano-seismic signals and evaluating the seismic wavefield properties (e.g., Chouet, 1996b). While most of the array-techniques are discussed in Chapter 9, we will focus on some results obtained when applying them in volcano monitoring and signal analysis.

The main deviation from typical array techniques in earthquake seismology is that the height differences between the array stations can not be neglected when the array is deployed on the flanks of a volcano. The effect of a 3D-distribution of stations can be minimized by fitting a plane to the station locations, which is possibly dipping according to the topography. One then transforms all auxiliary information (i.e., station coordinates) and refers all estimated parameters (incidence, azimuth and horizontal slowness) to this "best fitting plane".

13.4.4.1 f-k beamforming

One of the most useful properties of a seismic array is its capability for suppressing undesired signals by filtering the incoming wavefield in the spatial as well as in the frequency domain. Thus, we can estimate the coherence, the signal power, the azimuth and the apparent velocity of an incoming wave. Because most seismic signals map into different regions of the frequency-wave number plane (see, e.g., Figs. 9.28, 9.38 and 9.40), f-k beamforming is an excellent tool to distinguish between the different wave-types. Beamforming can be thought of as delaying each seismic trace in time such that waves will add constructively when summed. The delay times necessary to obtain maximum "beam-power" are used to determine the direction of wave propagation through the array. Beams "aimed" in a direction far from a source will add destructively and produce a low signal. If the seismic array is located some wavelength apart from the assumed source area, and the spatial extend of the array is small compared to the distance towards the source, we can also assume plane-wave propagation. Under these assumptions it is possible to estimate the backazimuth towards the source and, if the velocity model directly below the array is known, we can also estimate the incidence of the incoming plane wave. We can then invert for the source area of the signal (see 9.4.2 - 9.4.4).

Fig. 13.25 gives an example of a broadband f-k analysis with data recorded at Mt. Merapi. Obviously, only the very first part of the signal shows a phase with high coherence b), which additionally shows a small slowness c) (high apparent velocity). In contrast, later arrivals have randomly fluctuating backazimuth and slowness values. A possible interpretation of this pattern is that the recorded event consists of an array-wide coherent body phase (indicated by the high coherence and red color coding), which could be used for locating the event combining the backazimuth information and, if the velocity model just beneath the array is known, the incidence angle estimated from the slowness. This coherent phase is followed by randomly incident waves.

Thus, the potential of a seismic array to discriminate between various types of incoming seismic waves and to quantify their properties makes the f-k beamforming perhaps the most powerful tool for investigation of continuous signals (i.e., volcanic tremor). Furumoto et al. (1990) and Almendros et al. (1997) showed the results of tracking a volcanic tremor source in space and time using seismic array beamforming. Other applications of large seismic arrays

have been reported by Saccorotti et al. (1998), Chouet et al. (1997) and La Rocca et al. (2000), to name a few.

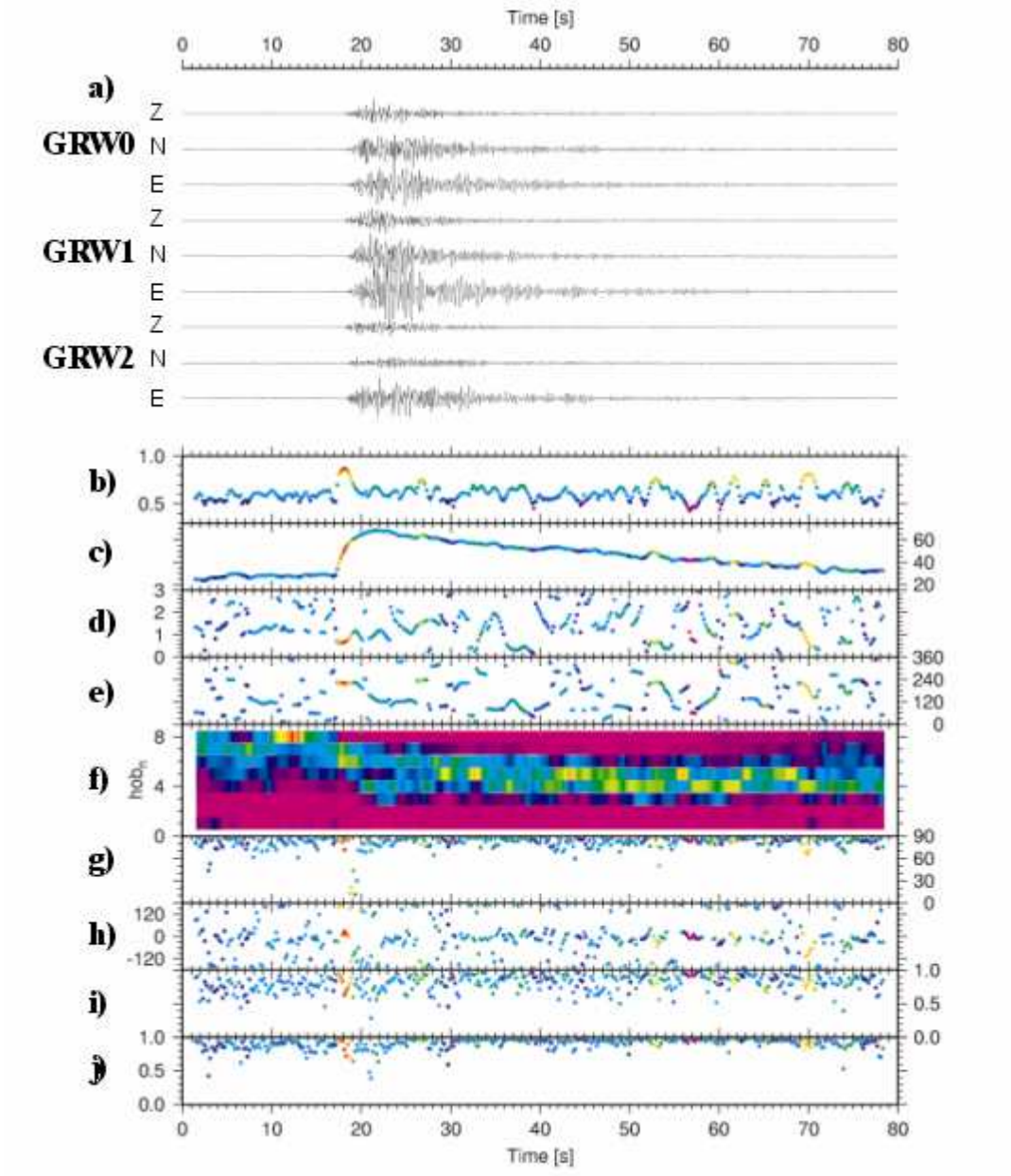

Fig. 13.25 Output of a continuous array analysis of a small seismic array with three component seismometers: a) shows the waveforms of a VT-B type event at the different seismometers; b) is the relative power (semblance) obtained by the f-k analysis; c) shows the overall power in the array in a dB scale while d) and e) give the slowness in s/km and the backazimuth in degree of the incoming waves, respectively. f) shows the array-wide averaged time-frequency pattern in 8 half octave bands; g) and h) show the incidence and azimuth of the array wide averaged polarization pattern (in degree), while i) is a measure of rectilinearity and j) is the planarity of the analyzed signal. The color coding of b) to e) and g) to j) is proportional to the highest semblance value obtained in this signal. The high coherent phase at the beginning of the signal can be used for beam steering towards the source location (courtesy of M. Ohrnberger, University of Potsdam).

However, the application of beamforming techniques in volcano monitoring requires high computer power, rarely available during a volcanic crisis. In order to reduce it, one can use the spatial filter properties of seismic arrays and apply the f-k beamforming to steer in one or several directions of special interest (similar to beamsteering used to detect underground nuclear explosions; see 9.6 and 9.7.7). Another way to reduce computational processing includes optimization of searching the maximum of the beam in the f-k plane (i.e., highest coherence value) by using simulated annealing and/or simplex techniques (Ohrnberger, 2001).

13.4.4.2 Array polarization

As three-component seismometers are becoming the standard instrument nowadays and seismic arrays consist frequently of large numbers of three axial sensors, it is also possible to evaluate the polarization properties of the whole array. While there is no straight-forward method to include the polarization properties directly into the f-k-algorithm, it is possible to estimate array-averaged parameters of the 3D-trajectories. Jurkevics (1988) showed that array-wide averaging of the covariance matrices (see 13.4.2.2) results in a more stable estimate of the seismic wave vector (see Fig. 13.22). Jurkevics (1988) also demonstrated the insensitivity of this estimate to alignment problems within the array. With this algorithm it is also possible to average the polarization properties over certain frequency bands which is a further link to the averaging properties of the broadband f-k-analysis (see 9.7).

A further method to incorporate three-component seismic recordings of an array is to compute the “waveform” semblance (e.g., Ohminato et al., 1998; Kawakatsu et al., 2000). This approach consists of a grid search over possible source locations and the simultaneous rotation of the 3D ground motion vector towards these hypothetical sources. The semblance value of the L direction is computed. The L-Q-T system is defined by the direction from the source to the station L, the plane Q perpendicular to L including the source and receiver, and the plane T perpendicular to Q. Assuming a source which generates solely a compressional wave in L direction, the energy-density on the orthogonal components should be zero. Finally the “waveform” semblance should be 1 if the signal is coherent on all array stations and no energy is left on the two directions perpendicular to L. On the other hand, the “waveform” semblance should be zero if there exists only incoherent wave-groups and/or there is still a signal on the components different to L. It must be emphasized that this approach is restricted to cases where path effects and the influence of the free surface have no, or vanishing, influence on the orientation of the particle motion, i.e., low-frequency near-field observations.

13.4.4.3 Hypocenter determination using seismic arrays

As described in the 13.4.4.1, it is possible to track seismic sources in space and time using seismic arrays. Unfortunately, the exact seismic velocity distribution of a volcano is not known. This results in large uncertainties in estimating the location of volcanic-seismic sources. One possible solution is to use not only one array but a network of arrays distributed around the volcano to compute the backazimuth of the coherent arrivals for each array separately and to invert them for the epicenter of the signal. Applications of this technique can be found in La Rocca et al. (2000).

Another difficulty arises when the seismic array is located close to the source and/or the height differences between the array stations are not negligible. Then, the usually assumed plane-wave propagation is no longer a good approximation and therefore the results are biased to an unknown extent, because neither the influence of the topography nor the deviation of the wavefront from a plane wave is exactly known. In this case, a better way to localize the seismic source is to apply a more complicated approach, which first uses f-k beamforming to detect coherent phases within the continuous seismic data records, and then to apply two-station generalized cross-correlation techniques in order to estimate the time difference of arrivals between the two stations. Wassermann and Ohrnberger (2001) successfully applied this technique to localize VT and strong MP events recorded at Mt. Merapi without the need of interactively determined onsets.

While this algorithm is only applicable to coherent and transient signals, algorithms exist which are based on the migration of coherent phases back to the source region (Almendros et al., 1999; Ohminato et al., 1998; Wassermann, 1997). Unfortunately, the computational load of these algorithms is high and their application is restricted to the "off-line" analysis of selected signals of special interest.

13.4.4.4 Classification problem using seismic arrays

When establishing a seismic array at an active volcano it is also possible to revise the classification scheme used. Besides the usually applied time-frequency analysis (see 13.4.1.1), we can also use wavefield properties obtained from the array analysis to enhance significantly our discrimination quality. Most recently Ohrnberger (2001) applied speech recognition techniques on parameters deduced from a continuous array analysis using data recorded at the Mt. Merapi volcano. Fig. 13.25 from Ohrnberger (2001) gives an example of the output of the continuous parameterization using seismic array techniques. The key point in this approach is the assumption that different signal types will show different wavefield properties (e.g., coherence, time-frequency behavior, polarization properties and absolute time-amplitude behavior).

13.4.5 Automatic analysis

During a seismic crisis or in the framework of a long-term seismic surveillance, it is not possible to apply all the analysis tools described above in a visually controlled, interactive manner. During the October 1996 volcanic crisis at Mt. Merapi, nearly 5000 events per day occurred. This large number of events obviously precludes any on-line, interactive analysis of the seismic data.

There are various approaches to automate at least some parts of the routine analysis in a volcanic observatory (e.g., Patanè and Ferrari, 1999). The most prominent software package is called Earthworm (Johnson et al., 1995), developed mainly under the auspices of the U.S.G.S. Many of the techniques described above are implemented in this "real-time" environment, e.g., continuous spectral analysis, RSAM, SSAM, automatic event associations, hypocenter location and magnitude. Mainly designed for monitoring local earthquakes, the widespread use at volcano observatories has led to the development of new, volcano related modules and promises new tools in the future. The Earthworm system appears to be very flexible and

capable of being adapted to special requirements at different volcanoes. However, the great flexibility of this software package entails rather complex and unwieldy setup procedures when establishing the system the first time.

The software for array analysis and some of the new tools for spectral analysis used in this Chapter were implemented into the Earthworm system and will be released after some beta-testing done through this year (2001).

13.5 Other monitoring techniques

As described at the beginning of this Chapter, seismology is generally seen as the most reliable and diagnostic tool for monitoring a restless or erupting volcano. However, data from seismological surveillance alone are inadequate to understand and forecast eruptions. Modern approaches to monitoring systems will therefore combine seismology with other geophysical, geochemical, geodetic and geological techniques. Below we focus on just a few of the various ground-based monitoring techniques that are closely related to seismology. We will not discuss the wide and fast-developing field of remote sensing in the volcanological context. For this we refer, as a good starting point, to Scarpa and Tilling (1996).

13.5.1 Ground deformation

Closely related to seismology is the monitoring of the deformation field caused by a magma injection and/or hydrothermal pressurization within the volcano's shallow or deep edifice. Deformation can be considered as an extension of seismology to lower, quasi-static frequencies. Modern techniques of monitoring the deformation signals of a restless volcano include borehole tiltmeters and/or strainmeters, *electronic distance meter* (EDM) networks and *Global Positioning System* (GPS) networks. Due to the increasing amount of GPS satellites and accuracy, GPS will play an important role in the field of ground deformation monitoring during the next decades.

The key point of this monitoring technique is the assumption that shallow or deep injection of large volumes of magma below a volcano will cause significant deformation of its surface. There were several successful approaches to forecast the 1980 eruption of Mt. St. Helens using deformation information (Murray et al., 2000) and at Hekla volcano, Iceland (Linde et al., 1993). The most recent 2000 eruption of the Hekla volcano was accompanied by significant signals recorded by a cluster of strain meters located around the volcano (http://hraun.vedur.is/ja/englishweb/heklanews.html#strain). In addition, shortly before the eruption, increasing seismicity and volcanic tremor led to a precise forecast of the following eruption (see Fig. 13.26). This can be seen as a perfect example of the interaction of two different monitoring techniques. In addition, there are many papers dealing with correlation between seismic signals and ground deformation at Kilauea volcano (Hawaii; e.g., Tilling et al., 1987).

A further example of a good correlation between measurable deformation and the appearance of seismic signals is known from Suffriere Hill volcano, Montserrat Island, West Indies, where Voight et al. (1998) observed a coincidence between several swarms of Hybrid events with cyclic changes in the deformation signals. This coincidence is very important regarding the inversion of source mechanisms of this class of signals. This kind of deformation signal,

in conjunction with magma intrusion into the volcanic edifice, is known to be very small and mainly related to the active part of the volcanic dome. At Mt. Merapi, several clusters of borehole tiltmeters are installed at the flanks, but only very weak signals have been recorded until now (Rebscher et al., 2000). In contrast, strong deformation signals are visible at the volcano's summit stations (Voight et al., 2000). This might indicate that at Mt. Merapi no large-sized and shallow-situated magma chamber exists and that the volume of ascending magma during typical eruptive phases is small. However, tilt stations at the flanks of Mt. Merapi and other volcanoes with apparent small magmatic activity are very useful for discrimination between the usual small magma intrusions and possible larger ascending volumes of magma, which should then produce a much more pronounced tilt signal.

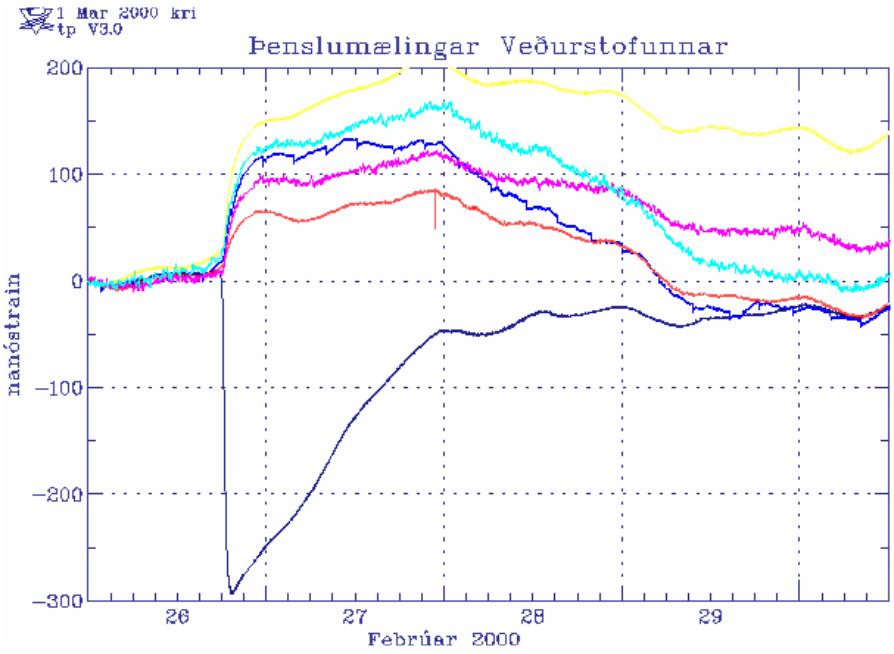

Fig. 13.26 The strainmeter data preceding the Hekla 2000 eruption are shown. As a result, three different phases could be defined. Firstly, a conduit was opened between 17:45 to 18: 17. Secondly, a reduced rate of expansion of the same conduit at 19:20 could be detected and finally all stations showed an increase when the conduit was fully opened and magma was flowing directly beneath the volcano (courtesy of Icelandic Meteorological Office, http://hraun.vedur.is/ja/englishweb/heklanews.html#strain).

13.5.2 Micro-Gravimetry

The appearance of gravity changes at an active volcano also reflect possible inflation/ deflation cycles of magmatic material. There is a complicated interaction between physical and geometric properties (i.e., density, volume, location) of the moving material and height changes caused by the deformation of the surface of a volcano. Therefore, the monitoring of gravity changes is a challenging task that should be carried out with great care. As height changes are generally the reason for gravity changes, gravity monitoring should always be combined with high precision leveling (e.g., EDM or GPS measurements). For a reliable and less ambiguous inversion of the gravity data, a good knowledge of the velocity structure of the volcano is needed. Models of the magmatic system from gravity data should be regarded with caution, unless the conclusions are also supported by other independent observations.

13.5.3 Gas monitoring

Another important parameter preceding a volcanic eruption is the volume, velocity, temperature and composition of the emitted gas from a volcanic vent or fumarole. Volatiles and released gases are seen as the most important driving forces for both an eruption and the source of volcanic signals (e.g., explosion quakes, LF, MP, volcanic tremor) (Schick, 1988; Vergniolle and Jaupart, 1990). Different techniques of gas sampling are in use, ranging from routinely collected gas samples in a weekly or monthly manner to a continuous analysis (every 20 - 30 min) of the emitted gas using a gas-chromatograph (Zimmer and Erzinger, 2001). The high sampling rate in continuous analysis at Mt. Merapi revealed surprisingly short period pulsations (with a duration of 5 hours to 3 hours; see Fig. 13.27) in the water to carbon-dioxide ratio as well as in the temperature of a fumarole (Zimmer and Erzinger, 2001). However, no significant correlation between this pulsation and the related seismicity could be found. Only the rhythms in this pulsating gas source were changed when the number of very shallow MP-events also increased. This lack of correlation of fast sampled gas data and seismic signals at Mt. Merapi might be caused by our imperfect knowledge of how to parameterize the seismicity and the gas composition, respectively. Several case studies of changes in the chemical composition of fumarolic gases, including descriptions of the accompanying seismicity and ground deformation, is given by Martini (1996).

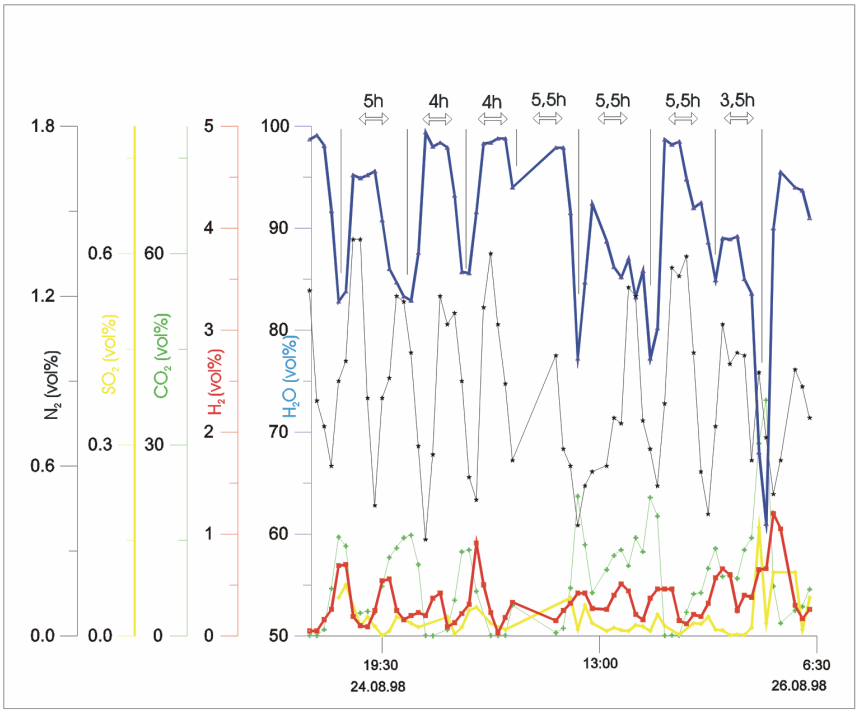

Fig. 13.27 Variation of the gas composition at one of Mt. Merapi's fumaroles. The gas is automatically analyzed approximately every 30 min using a gas-chromatograph. The analysis shows a fast changing composition of the gas with a period of roughly 5 hrs (courtesy of M. Zimmer, GeoForschungsZentrum Potsdam).

Many other papers deal with the long term variations of gas prior to a volcanic eruption, which makes this technique a useful tool for long term monitoring (e.g., Stix and Gaonac'h, 2000).

13.5.4 Meteorological parameters

While not directly linked to the eruptive behavior of a volcano, monitoring meteorological conditions is important for the proper interpretation of observed parameters as well as for the anticipation of possible triggering of volcanic activity. Lahars, i.e., volcanic debris flow, are often triggered by heavy rainfall which additionally weakens the unconsolidated volcanic material. At Mt. Merapi, small-size gravitational dome collapses take place more frequently during the tropical rainy season.

The influence of meteorological conditions on the installed monitoring equipment is manifold. Barometric pressure and temperature changes could cause severe disturbances on installed broadband seismometers and tiltmeters, respectively. While these influences can be reduced by proper installation of the sensors (see 13.6), they are never completely removed. Spectral analysis of both meteorological and surveillance parameters may help to identify possible disturbances of the installed sensors. As mentioned before, rainfall may trigger volcanic as well as seismic activity. A good monitoring station will therefore also have a continuously recording rain gauge.

In order to better judge the influence of meteorological (and also tidal) effects on the sensors and/or the volcanic activity, continuous long-term meteorological recordings are needed. Frankly speaking, this is a difficult and sometimes impossible task because of the harsh environments at many active volcanoes. However, the continuity of such measurements are among the most important functions of a volcano observatory.

13.6 Technical considerations

13.6.1 Site

After selecting a possible site (see 3.1) for a seismic station or a seismic array, much care should be taken to protect the sensor from meteorological and other external effects. In Fig. 13.28a, a sketch of a possible installation scheme is shown. If a broadband sensor is to be deployed, extra care must be taken to protect this sensitive sensor from temperature and barometric pressure influences (see 5.5 and 7.4).

The weather conditions at volcanoes at even moderate altitudes can be very rough and may change rapidly. Protection against rain and lightning is the most important task when constructing a seismic station. All equipment should be placed in water tight casings. Lightning protection is the most important and, unfortunately, the most difficult problem to solve (see 7.4.2.5). Usually, volcanoes have high resistivity surface layers (ash, lapilli etc.), making a proper grounding of the instruments nearly impossible. One of the optimal techniques to protect the equipment against lightning damage is to install a tower in the vicinity of the station with a mounted copper spire on top. The tower should be grounded as much as possible and connected entirely with the ground of the power-sensitive equipment.

Furthermore, lightning protectors should be placed in front of any equipment to reduce the effect of high-voltage bursts (see Fig. 13.28b-c). Long cable runs should be avoided or changed to fibre optics. Using fibre optic cables for signal transmission also has the advantage of being insensitive to electro-magnetic effects, which sometimes cause spike bursts on the

transmitted signals.

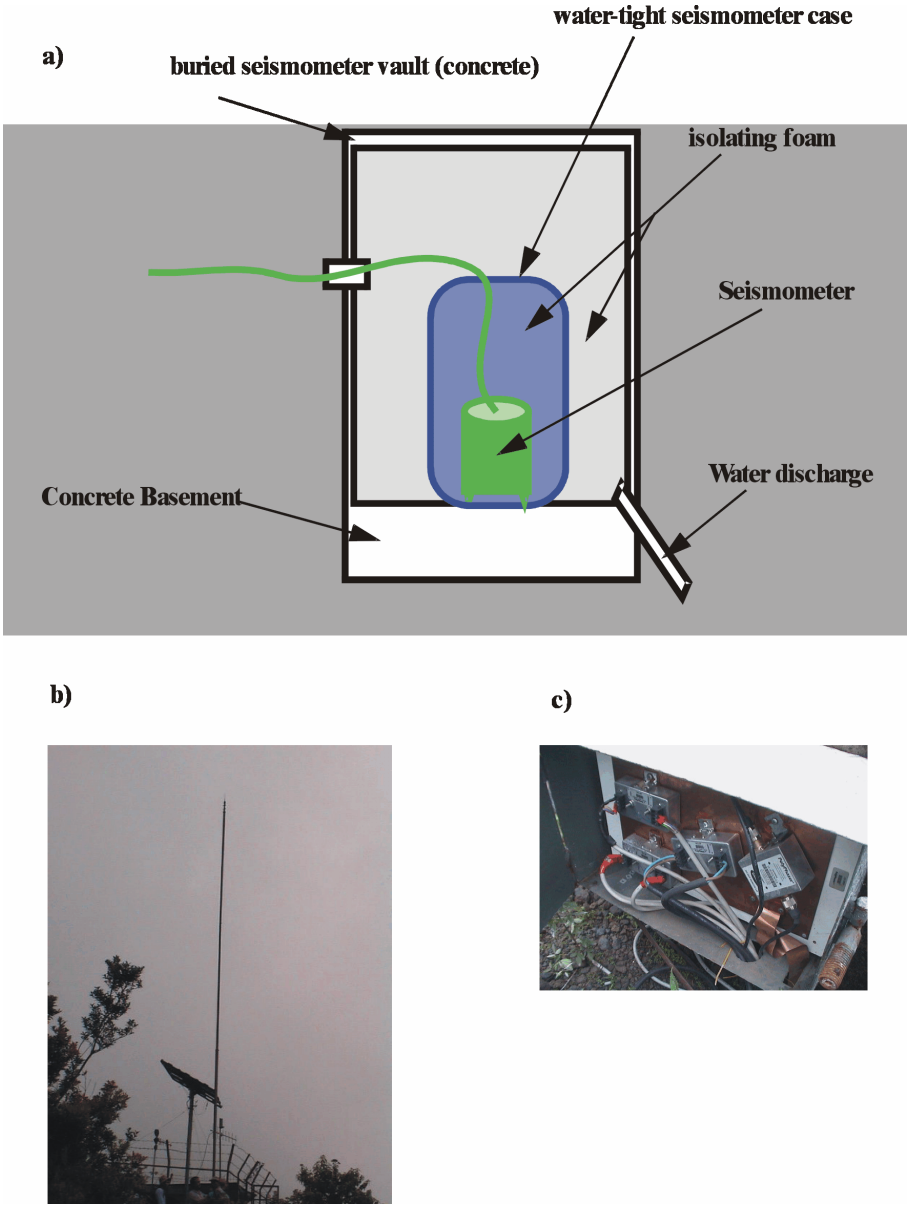

Fig. 13.28 a) Sketch of a seismometer vault: the sensor should be placed in a water tight casing which is placed firmly on a concrete basement. In order to isolate the sensor against temperature and pressure changes due to air turbulences, the void space should be completely filled with insulating rubber foam or similar (see 7.4.2); b) shows a lightning tower installed at Mt. Merapi, while c) shows additional lightning protectors for all sensitive equipment. The copper plate and all external devices (photo-voltaic modules) should be connected to the lightning tower.

13.6.2 Sensors and digitizers

Because the seismic signals produced by an active volcano cover a wide dynamic range, the choice of the digitizer, i.e., the needed dynamic range, should be carefully evaluated. Modern digitizers will sample the analog seismometer output with 24 bit resolution which results in a

dynamic range of roughly 136 dB (depending on the sampling rate). A 16 bit A/D converter would usually be sufficient, but eruptive phases with various large amplitude signals will then saturate the digitizers' dynamic range (e.g., pyroclastic density flows, big explosions etc.). So called "gain-ranging" (i.e., the pre-amplification will be lowered if the signal is getting stronger) should be avoided because it will result in lower resolution and might mask small but important signals. Best suited are digitizers which sample with 24 bit resolution but store the data depending on the recorded peak amplitude (i.e., 8 bits are stored if the signals are small and the activity is low, 16 bits when the activity is increasing and 32 bits if high activity occurs and the full 24 bit range is used).

If a network of seismic sensors is planned, several three-component short-period instruments (i.e., with 1 Hz corner frequency) will be sufficient (see 13.3.2). If the near-crater range is accessible, installing one or two broadband stations (i.e., 0.00833 to 0.05 Hz corner frequency) will be a good choice. If large (M>4) earthquakes from an active volcano flank or nearby fault or subduction zone are possible, some broadband stations are preferred.

If an array or a network of arrays is to be installed, a mixture of three-component broadband and short-period one-component seismometers will be sufficient (especially when realizing that there is no straight-forward technique available which includes directly 3D seismic array data).

13.6.3 Analog versus digital telemetry

Most of today's established monitoring networks at volcanoes are designed for transmitting the data "on-line" to a central data center, generally the local volcano observatory. This might be the main technical difference between a short-term seismological experiment and the long-term monitoring of a volcano. From worldwide experience, establishing a reliable radio line is a difficult and time-consuming task, which is also subject to change when new telecommunication facilities are constructed nearby and possibly worsen the data communication.

There are large differences between analog and digital radio transmission regarding data rate, dynamic range and sites to be selected and distance ranges to be covered. If a high resolution is required (e.g., using a 24 or 16 bit A/D converter at the sensor), the only way to exploit the full bandwidth of data is to transmit the signals with a digital radio modem. Meanwhile, several companies offer spread-spectrum modems which transmit in the frequency range of roughly 1 GHz and 2 GHz, respectively. The big advantage of these digital modems is the high data throughput (115,200 baud) and the low power consumption (transmitting power roughly 1 Watt). On the other hand, the high transmission frequency is the main drawback of the digital radios. As a rule, the station and the data center must be in direct line of sight, with no hills, trees or other obstacles between them. This limitation should also be kept in mind when selecting a suitable seismic station site. The problem of obstacles can be circumvented when installing several repeaters on the way to the data center. Even so, the network design depends on intended radio lines (see also 7.3 and Information Sheet IS 8.2).

A disadvantage of analog radio communication is the limited dynamic range and data throughput (usually below 38,400 baud). Most of the installed analog radio systems are barely able to transmit 12 bits and, therefore, the signals must be bandpass filtered (e.g., 1 - 20 Hz) before transmitting. This is not acceptable when installing a broadband sensor. On the other

hand, radios are cheap and the typical frequency bands (100 MHz or 400 MHz) will enable a solid radio link even when the stations are slightly “out of sight”.

13.6.4 Power considerations

Most of the stations will be remote and no access to a power network will exist. Therefore, the first step is to calculate the expected power consumption of the seismic station. This will strongly depend on the kind of digitizer and sensor used, whether the data are transmitted by radio or not and which options for local data storage are desired. Therefore the power consumption of the field equipment should be extensively tested in the lab before constructing the power supply at the site and deploying the instruments. Never trust the optimistic specifications given by the manufacturer!

Most likely the power will be delivered by photo-voltaic (PV) modules where a variety of different systems is available. All components of a monitoring installation must fit together, including the capacity of batteries and solar charger. Care must be taken when estimating the amount of solar-modules needed to supply the stations. As a rule of thumb, 10% of the nominal maximum voltage will be supplied by the panels on average (i.e., using a 50 Watt module just 5 W are available on average). Voltage will typically decrease when the panels are installed high up in the mountains. Clouds, snow or ashfall may further reduce the effective power output (i.e., 5% or even less). This significantly increases the number of PV-modules required. To give an example: if the station consumes at least 20 W (including radio, some digitizers, SCSI disks for local storage etc.), you will need 400 W panel power which in the worst case is 8 x 50 W panels at this station!

Also the capacity of the battery must be adequate in case no solar power is produced. On the other hand, the battery should not be too big in capacity as the PV-modules must be able to recharge the battery in sufficient time. Whenever possible, alternative power sources should be used, such as robust wind generators. In case the station is located near running water, a small hydro-power engine could be a good alternative.

13.6.5 Data center

All data streams, including those from monitoring techniques in addition to seismic, should be collected, stored and archived in a central facility. In the age of high-performance low-cost PC’s, few standard computers will be sufficient to satisfy all needs of data collection, backup systems, automatic and visual analysis. Because continuous recording of all relevant signals is preferred over triggered data, a good backup strategy is crucial for getting complete and long-term data. Continuous recording is indispensable for improving our knowledge about volcanic activity, the underlying physical mechanisms and the relevant parameters to be observed when aiming at improving eruption forecasting. With the advent of DVD disks and CD-ROMS a good solution would be to write images of data sets onto one of these media in a daily or regular manner. CD-ROMS in particular assure a good data safety to price ratio.

Much public domain software is available for either automatic (e.g., Earthworm; Johnson et al., 1995) or interactive analysis (SeismicHandler, SAC, IASPEI-Software, PITSA/GIANT). The Orfeus homepage is a good starting point when looking for suitable software and for further contacts (see http://orfeus.knmi.nl/).

A special requirement of the data center is the availability of an "uninteruptable power supply" (UPS) to guarantee a loss-less data collection even if the power line of the observatory is broken. Depending on the quality of the power network, a generator could be a good solution to bypass blackouts which may last several hours.

Establishing a "quick-response" volcano observatory during a volcanic crisis of a long-dormant volcano needs additional equipment and design criterea of the monitoring network to be deployed. All equipment, including the data center facilities, should be lightweight, robust and low power consuming. This demands possible down-grades in resolution and data throughput. A comprehensive description of one realization of mobile monitoring networks is given in the *Mobile Volcano-Monitoring System* by Murray et al. (1996).

Acknowledgments

I am grateful to the reviewers F. Klein, R. Scarpa and R. Tilling for their helpful comments and corrections which improved the text significantly. I also thank P. Bormann for additional editing of this Chapter. Furthermore, figures and seismograms provided by E. Gottschämmer, S. Falsaperla, S. McNutt and M. Ohrnberger, are highly appreciated.

Recommended overview readings (see References, under Miscellaneous in Volume 2)

Civetta, L., Gasparini, P., Luongo, G., and Rapolla, A. (Eds.) (1974).
McNutt (2002)
Newhall, C. G., and Punongbayan, R. S. (Eds.) (1996).
Scarpa, R. and Tilling, R. (Eds.) (1996).
Sigurdsson, H. (Ed. in Chief) (2000).